JOURNAL OF VIROLOGY, Mar. 2002, p. 2936–2951 Vol. 76, No. 6
0022-538X/02/$04.00+0 DOI: 10.1128/JVI.76.6.2936–2951.2002

Infectious and Whole Inactivated Simian Immunodeficiency Viruses Interact Similarly with Primate Dendritic Cells (DCs): Differential Intracellular Fate of Virions in Mature and Immature DCs

I. Frank,[1]† M. Piatak, Jr.,[2] H. Stoessel,[3] N. Romani,[3] D. Bonnyay,[1] J. D. Lifson,[2] and M. Pope[1]*

Laboratory of Cellular Physiology and Immunology, The Rockefeller University, New York, New York, 10021[1]; Retroviral Pathogenesis Laboratory, AIDS Vaccine Program, SAIC-Frederick, National Cancer Institute at Frederick, Frederick, Maryland 21702[2]; and Department of Dermatology and Venereology, University of Innsbruck, Innsbruck, Austria[3]

Received 22 June 2001/Accepted 18 December 2001

As potential targets for human immunodeficiency virus type 1 and simian immunodeficiency virus (HIV-1 and SIV), dendritic cells (DCs) likely play a significant role in the onset and spread of infection as well as in the induction of antiviral immunity. Using the SIV-macaque system to study the very early events in DC-virus interactions, we compared chemically inactivated SIV having conformationally and functionally intact envelope glycoproteins (2,2′-dithiodipyridine [AT-2] SIV) to infectious and heat-treated SIV. Both human and macaque DCs interact similarly with SIV without detectable effects on DC viability, phenotype, or endocytic function. As assessed by measuring cell-associated viral RNA, considerable amounts of virus are captured by the DCs and this is reduced when the virus is heat treated or derived from a strain that expresses low levels of envelope glycoprotein. Immunostaining for SIV proteins and electron microscopy indicated that few intact virus particles are retained at the periphery of the endocytically active, immature DCs. This contrasts with a perinuclear localization of numerous virions in large vesicular compartments deeper within mature DCs (in which macropinocytosis is down-regulated). Both immature and mature DCs are capable of clathrin-coated pit-mediated uptake of SIV, supporting the notion that the receptor-mediated uptake of virus can occur readily in mature DCs. While large numbers of whole viruses were preferentially found in mature DCs, both immature and mature DCs contained similar amounts of viral RNA, suggesting that different uptake/virus entry mechanisms are active in immature and mature DCs. These findings have significant implications for cell-to-cell transmission of HIV-1 and SIV and support the use of AT-2 SIV, an authentic but noninfectious form of virus, as a useful tool for studies of processing and presentation of AT-2 SIV antigens by DCs.

Dendritic cells (DCs) appear to play a central, multifaceted role in the biology of human immunodeficiency virus type 1 (HIV-1) and simian immunodeficiency virus (SIV) infections. This role is facilitated by virtue of DCs being one of the initial cell lineages involved in virus transmission to a new host, through their ability to capture HIV and SIV and to transmit infection to $CD4^+$ T lymphocytes with unparalleled efficiency and through their key role as antigen (Ag)-presenting cells (APCs) in the induction of antiviral immune responses (27). Therefore, it is critical to delineate the biology of DC-virus interplay to better understand why virus replication predominates over effective antiviral immunity in the DC–T-cell milieu and how the DC-virus interactions can be exploited to optimize Ag presentation in DC-based vaccine and immunotherapeutic settings. The SIV-macaque system represents one of the best animal models available to study these events (10).

Bone marrow-derived DCs are a distinct group of APCs that capture Ags and efficiently activate specific naive and memory T-cell and B-cell responses (4). Typically, immature DCs have abundant endocytic capacity but not optimal Ag-presenting ability. In contrast, upon maturation DCs show a lessening of endocytic activity, with enhanced Ag presentation and immunostimulatory function (4). DCs can take up molecules via a number of mechanisms, including phagocytosis, macropinocytosis, and receptor-mediated endocytosis via clathrin-coated pits or caveolae (33, 47, 54). While macropinocytosis drastically diminishes in mature DCs, the numbers of clathrin-coated pits and vesicles are unaltered, suggesting that uptake via this mechanism may be maintained upon maturation, as seen with DEC-205 (CD205) (29, 34) and transferrin (TF) receptor (CD71) (15).

Myeloid DCs derived from the blood, skin, or mucosae of rhesus macaques appear to exhibit most features that have been described for their human counterparts (5, 23, 24, 27, 37, 38, 42). As has been described in the human setting (14, 30), mature monocyte-derived macaque DCs are most reliably obtained by exposing cultured monocytes to a cocktail of inflammatory factors, including prostaglandin E_2 (PGE_2), tumor necrosis factor alpha (TNF-α), interleukin-1β (IL-1β), and IL-6 (37). In particular, cocktail-matured human and macaque DCs exhibit a reproducibly uniform phenotype, enhanced viability, and potent immunostimulatory capacities, while maintaining their endocytic capacity via receptor-mediated uptake mechanisms.

Macaque DCs are also comparable to their human counterparts in how they interact with SIV. Macaque DC–T-cell mixtures favor virus replication (25, 42). This cellular environment is analogous to sites where HIV-1 and SIV can replicate in vivo (27) and, thus, provides a biologically relevant in vitro system to dissect the early DC-virus interactions involved in virus

* Corresponding author. Present address: Population Council, Center for Biomedical Research, 1230 York Ave., New York, NY 10021. Phone: (212) 327-7794. Fax: (212) 327-7764. E-mail: mpope@popcbr.rockefeller.edu.

† Present address: Population Council, Center for Biomedical Research, New York, NY 10021.

replication and immune activation. In vivo work further suggests that DCs within the mucosae may be one of the first cell populations targeted by the virus in transmission to a new host (22) and thereby may be pivotal for the spread of infection and amplification of viral replication in $CD4^+$ T cells (49, 57). Prior work has detailed the involvement of CD4, chemokine receptors, and DC-SIGN (CD209) in the capture and amplification of infection in the DC–T-cell milieu (27). The modulation of such molecules during DC differentiation as well as their selective expression on certain DC subsets (e.g., CD209 is not expressed by the DCs in the outer epithelia of the mucosae [16, 17]) underscores that DC-virus interactions are likely very complex. To date, direct visualization of early DC-virus interactions has been limited (8, 21). Thus, close examination is necessary to appreciate these crucial early events driving the capture of virus and spread throughout the immune system.

For such studies we have utilized a novel, recently developed type of chemically inactivated whole SIV. Treatment of HIV-1 or SIV with 2,2′-dithiodipyridine (aldrithiol-2 [AT-2]) results in preferential covalent modification of free thiol groups on virion internal structural proteins, including the cysteines of the zinc finger motifs of the nucleocapsid protein (18), thereby rendering the virus noninfectious, while preserving the conformational and functional integrity of the surface proteins, such as the envelope glycoproteins, in which cysteine residues are disulfide bonded (2, 45). Such treated virus preparations (AT-2 SIV and HIV-1) bind to surface molecules of T cells in an authentic manner and induce CD4-dependent cell-cell fusion, highlighting the value of this system for studying the cell-virus interactions. In particular, the use of noninfectious virions capable of authentic interactions with target cells facilitates evaluation of cell-virus interactions in the absence of potentially confounding effects of productive infection. The ability to pulse DCs with relatively large amounts of virus also allows the location and fate of the virus in these sentinel cells to be visualized.

The studies described herein are the first direct comparison of immature and mature human and monkey DCs revealing that the capture and uptake of AT-2 SIV by immature and mature primate DCs mirror the handling of infectious, native SIV. Mature DCs efficiently internalize structurally intact virus, even though macropinocytosis is dramatically decreased in these cells. Notably, the virus taken up by the mature DCs is located in large perinuclear vesicles. In contrast, fewer intact virions are taken up by the endocytically active immature DCs and remain close to the plasma membrane. Although there are striking differences in the intracellular fate of the virions, the level of viral RNA captured by immature versus mature DCs is comparable and if anything is slightly greater in immature DCs. Hence, while both DC populations entrap virus, they appear to handle it quite differently. Studies are ongoing to define in detail the intracellular disposition of virions in both DC subpopulations and the implications of these observations for infection and cell-to-cell transmission, as well as induction of antiviral immune responses.

MATERIALS AND METHODS

Animals. Adult male and female rhesus macaques (*Macaca mulatta*) used in this study were housed at the Tulane Regional Primate Research Center and tested negative by PCR for simian type D retroviruses and for antibodies (Abs) to SIV, as well as simian T-cell leukemia virus. Animal care operations were in compliance with the regulation detailed under the Animal Welfare Act and in the "Guide for the Care and Use of Laboratory Animals."

Culture medium and reagents. The medium used throughout was complete RPMI (cRPMI) 1640 (Cellgro; Fisher Scientific, Springfield, N.J.) supplemented with 2 mM L-glutamine (GIBCO-BRL Life Technologies, Grand Island, N.Y.), 50 μM 2-mercaptoethanol (Sigma Chemical Co., St. Louis, Mo.), 10 mM HEPES (GIBCO-BRL Life Technologies), penicillin (100 U/ml)-streptomycin (100 μg/ml) (GIBCO-BRL Life Technologies), and 1% heparinized human plasma. Fetal calf serum (10%) (Sigma) was used for the culture of cell lines. Recombinant human (rh) IL-4, IL-1β, and IL-6 and rh TNF-α were purchased from R&D Systems (Minneapolis, Minn.), rh granulocyte-macrophage colony-stimulating factor (GM-CSF) was bought from Immunex (Seattle, Wash.), and PGE_2 (P6532) was ordered from Sigma. Fluorescein isothiocyanate-labeled dextran (FITC-DEX) (M_r = 40,000) and ALEXA-TF (ALEXA Fluor 488) were purchased from Molecular Probes, Inc. (Eugene, Oreg.).

Viruses. The live and AT-2-inactivated SIV preparations used in this study were generously provided by Julian Bess and Larry Arthur of the AIDS Vaccine Program (SAIC-Frederick, National Cancer Institute at Frederick, Frederick, Md.). Chemically inactivated noninfectious SIV with conformationally and functionally intact envelope glycoproteins was produced by treatment with AT-2 as described elsewhere (2, 45). Briefly, SIVmneE11S was obtained from supernatants of the cloned E11S cell line (6). Wild-type SIVmac239 was generously provided by Ron Desrosiers, Harvard Medical School. A molecularly engineered variant of SIVmac239 ("SIVmac239/251 tail") contained a stop codon in the envelope glycoprotein-coding sequence at position 734, resulting in truncation of the transmembrane (TM) envelope glycoprotein and the presence of high levels of subunit (SU) and TM on virions (generously provided by James Hoxie, University of Pennsylvania; Hoxie et al., unpublished). Both viruses were grown in the CEMx174 cell line. For chemical inactivation, virus was treated with 1 mM AT-2 (Aldrich, Milwaukee, Wis.) for 18 h at 4°C. Preparations of both native and AT-2-treated virus were produced by sucrose gradient banding in a continuous-flow centrifuge. Banded virus was then pelleted and resuspended to 1,000 times the original concentration. Sucrose gradient banding, pelleting, and resuspension served to purify and concentrate virus preparations and for the AT-2-treated virus to remove any residual unreacted reagent. The virus content of purified concentrated preparations was determined with an Ag capture immunoassay for the SIV Gag p27 Ag (AIDS Vaccine Program). Virus stocks were diluted in 1% bovine serum albumin (BSA) (Intergen, New York, N.Y.) in phosphate-buffered saline (PBS) and were stored as aliquots (3 μg of p27 Ag equivalent/ml) at −80°C until use. For heat denaturation, frozen aliquots of infectious or AT-2-treated virus (same virus batch) were thawed and incubated at 56°C in a water bath for 1 h with frequent mixing. Virus was then kept on ice until use (within 2 h) or stored at −80°C.

Preparation and culture of cells. Human and macaque DCs were generated from a highly enriched population of $CD14^+$ cells as previously described (26). Briefly, peripheral blood mononuclear cells were isolated from either heparinized human blood from healthy lab donors or leukopaks obtained from the New York City Blood Bank or from heparinized macaque blood using a Ficoll-Hypaque density gradient (Amersham Pharmacia Biotech AB, Uppsala, Sweden). $CD14^+$ cells were separated by positive selection using a magnetic cell-sorting system (Miltenyi Biotech, Auburn, Calif.) and were placed into six-well tissue culture plates (Becton Dickinson, Mountain View, Calif.) at 10^6 cells/ml in 3 ml of cRPMI medium. The cells were cultured for 6 days in the presence of 100 U of IL-4/ml and 1,000 U of GM-CSF/ml to generate immature DCs. Every 2nd day, cells were fed with the same amount of cytokines in 200 μl of cRPMI. To generate mature DCs, either 50% of the culture medium was replaced with monocyte-conditioned medium (MCM) (26) or 200 μl of cRPMI per well containing a cocktail of four factors was added, and the cells were cultured for two additional days. The cocktail included the following factors at the indicated final concentrations: IL-1β (10 ng/ml), IL-6 (1,000 U/ml), TNF-α (10 ng/ml), and PGE_2 (1 μg/ml). Immature (maintained in IL-4 and GM-CSF) DCs and mature DCs were then harvested on day 8.

Characterization of DCs by flow cytometry. The phenotype of immature and mature DCs was routinely monitored by two-color flow cytometry using FITC-conjugated mouse Ab against HLA-DR (Becton Dickinson) combined with a panel of phycoerythrin (PE)-conjugated mouse anti-human monoclonal Abs (MAbs). The following MAbs were used: anti-CD25, -CD80, -CD86 (all Becton Dickinson), and -CD83 (PN IM2218; Immunotech-Beckman-Coulter, Marseille, France). To evaluate the purity of DC populations, cells were also stained with anti-CD2 (MT910; DAKO, Glostrup, Denmark) to identify T cells and with anti-CD20 (Becton Dickinson) for B cells. To analyze the presence of coreceptors for HIV-1 and SIV, PE-conjugated anti-CXCR4 (PharMingen) and anti-CCR5 MAbs were used (anti-human CCR5 MAb from PharMingen and an

anti-human CCR5 MAb [clone 45531] reactive with macaque cells from R&D Systems). Isotype controls (FITC-immunoglobulin G1 [IgG1] and PE-IgG2a; Becton Dickinson; and PE-IgG2b; R&D Systems) were included for all Ab staining experiments. Cells were resuspended in PBS containing 5% fetal calf serum and 0.1% sodium azide (staining buffer) and were incubated (2×10^4 cells/well) with Abs in V-bottomed 96-well plates (ICN Biomedicals, Aurora, Ohio). After incubation for 20 min at 4°C, the cells were washed with staining buffer and fixed with 3.7% formaldehyde in PBS. Specimens were examined using a FACScan flow cytometer (Becton Dickinson, San Jose, Calif.), and acquired data were analyzed using CellQuest software.

Loading of DCs with AT-2 SIV. Up to 10^6 immature or mature human or monkey DCs were placed into 1.5-ml Eppendorf tubes and were incubated with infectious, AT-2, or heat-treated SIV diluted in cRPMI (0.5 to 3 ng of p27 Ag/10^4 cells) in a total volume of 100 μl at 4°C or 37°C for different lengths of time. Control cells were incubated with the equivalent amount of buffer (1% BSA in PBS) in cRPMI. After each incubation step the DCs were extensively washed using a refrigerated microfuge (3,000 rpm for 3 min) (centrifuge 5417 C/R; Eppendorf, Hamburg, Germany). This was repeated four times; each time the cells were resuspended in 500 μl of cold cRPMI or serum-free RPMI. The numbers of viable cells were counted by trypan blue exclusion, and pelleted aliquots (1×10^5 to 3×10^5 DCs) were stored under dry conditions at −80°C for RT-PCR analysis. Fractions of the remaining cells were used for fluorescence-activated cell sorter (FACS) and electron microscopy analysis, as well as immunostaining for SIV proteins.

RT-PCR analysis. Following various incubations of DCs with virus (infectious, AT-2-treated, and infectious or AT-2 SIV preparations subjected to heat treatment), cell-associated SIV genomic RNA was measured using a quantitative real-time RT-PCR assay. To do this, RNA was first prepared from cell pellets by digestion with 400 μg of proteinase K/ml to ensure complete release of RNA from AT-2-treated virus. Cell pellets were treated with 100 μl of Tris-buffered saline (Sigma) supplemented to contain 400 μg of proteinase K/ml, 0.2% sodium dodecyl sulfate, and 5 mM EDTA (Sigma). Samples were incubated at 55°C for 1 h with occasional vortexing. Proteins were then removed with two sequential extractions with an equal volume of phenol:chloroform:isoamyl alcohol (25:24:1), equilibrated with 10 mM Tris, pH 8.0, and 1 mM EDTA and supplemented to contain 0.05% hydroxyquinoline, followed by extraction with an equal volume of chloroform. One hundred micrograms of glycogen carrier was added, and total nucleic acid was precipitated by addition of 2.5 volumes of ethanol. Samples were stored overnight at −20°C. Precipitates were then pelleted by centrifugation at $16{,}000 \times g$ for 30 min at 5°C, rinsed by addition of 70% ethanol and recentrifugation for 15 min, drained of all ethanol, and dissolved in 100 μl of Molecular Biology-grade water. Quantitative reverse transcriptase PCR (RT-PCR) analysis for SIV *gag* sequences was then performed on 10-μl aliquots as described previously (32). Statistical analysis was performed with Student's *t* test for paired samples. The percentage of DC-captured virus was calculated based on the amount of input virus, which was set as 100%.

Cell fusion assay. DCs were pulsed (as described above) with infectious, AT-2-treated, or heat-treated (infectious or AT-2-treated) SIV for 2 h at 37°C, washed, and added to untreated CEMx174 cells (10^5) in a 96-well flat-bottomed plate (Falcon; Becton Dickinson Labware, Franklin Lakes, N.J.) (200 μl/well) at a DC-to-CEMx174 cell ratio of 1:10. Buffer-treated DCs were included as the control. In parallel, CEMx174 cells were cultured directly with the indicated amounts of cell-free AT-2 SIV. After virus- or buffer-treated DCs (versus cell-free virus) were cocultured with untreated CEMx174 cells for 2 to 3 h at 37°C, cytospins were prepared as previously described (38). Briefly, 2.75×10^4 cells (50 μl) per slide were loaded onto glass slides and spun in a cytocentrifuge (Shandon, Pittsburgh, Pa.) for 3 min at 900 rpm. Slides were then air dried for at least 1 h before being fixed in fresh acetone (Fisher Scientific). To more easily identify SIV-induced multinucleated giant cells (MGCs), specimens were stained with Giemsa (EM Science, Gibbstown, N.J.) according to the manufacturer's protocol. Syncytia were counted using a light microscope, and the whole spot of cells was screened for syncytia at a magnification of ×40. A profile containing more than two nuclei was considered a syncytium/MGC.

FACS analysis for endocytic function. DCs (5×10^5) were resuspended in 100 μl of buffer or buffer-containing AT-2 SIV (1.5 ng of p27 Ag/10^4 cells) in 1.5-ml Eppendorf tubes and were incubated at 37°C. After 30 min, 10 μl of medium or medium-containing FITC-DEX (20 μg/ml) or ALEXA-TF (20 μg/ml) was added and the cells were incubated for a further 30 min at 37°C. After a total incubation of 60 min, the cells were washed five times with cold medium and fixed with 3.7% formaldehyde, and the amount of accumulated fluorescent probes was monitored using a FACScan flow cytometer (Becton Dickinson). For some experiments, aliquots of tracer-loaded unfixed cells were adhered to slides and analyzed for intracellular SIV p27 Ag expression (see below).

Fluorescent staining of cytospins. Cytospins of untreated human immature and mature DCs were prepared (see above). Air-dried slides were fixed with acetone and exposed in sequence to the following Abs: a MAb directed against anticlathrin heavy chain (clone X-22, mouse IgG1; kind gift of F. M. Brodsky, UCSF), biotinylated donkey anti-mouse Ig (Pharmacia Amersham, Amersham, United Kingdom), and streptavidin Texas red (Amersham). Specimens were mounted in Vectashield (Vector Labs, Burlingame, Calif.) and were viewed by using a conventional fluorescence microscope.

Immunofluorescence microscopy: p27 staining. Cells were adhered to microscope slides (Carlson Scientific, Inc., Peotone, Ill.) that had been precoated with 1 mg of alcian blue (8GX; Sigma)/ml. For this, slides were boiled for 30 s in a water-diluted alcian blue solution, air dried, rinsed with water, and air dried again before slides were stored at room temperature. For adherence, virus- or buffer-treated DCs were resuspended in plasma-free medium, seeded ($\sim 2.5 \times 10^4$ cells/35 μl/well) onto pretreated slides, and incubated for 8 min at 4°C. Adhered cells were washed twice with cold PBS and were fixed in 4% fresh paraformaldehyde (PFA; Electron Microscopy Sciences, Fort Washington, Pa.) in PBS for 20 min at room temperature. To identify DCs carrying the infectious or AT-2 SIV, adherent cells were immunostained with the primary mouse MAb KK64 (IgG1), which reacts with SIV p27 *gag* protein (amino acids 151 to 180). For signal amplification of Ab-labeled cells, the TSA (Tyramid Signal Amplification) kit carrying the fluorophore FITC or cyanine 3 was used (NEN Life Science Products, Boston, Mass.) following the manufacturer's instructions. Where necessary, slide contents were incubated with 0.3% H_2O_2 for 60 min at room temperature after fixation to block endogenous peroxidase activity and were washed for 5 min in wash buffer. To reduce nonspecific signals, cells were incubated with blocking reagent provided with the TSA kit supplemented with 0.05% saponin (Calbiochem, San Diego, Calif.) for permeabilization. Saponin-containing blocking buffer was also used to dilute Abs. Between incubation steps, the cells were washed thoroughly with PBS–1% BSA. All steps were performed at room temperatures. After blocking, the KK64 MAb directed against p27 Ag (1:1,000) or the isotype control (IgG1; 5 μg/ml) was added for 30 min, followed by a 30-min incubation with a horseradish peroxidase (HRP) affinity-purified $F(ab')_2$ donkey anti-mouse Ig (DAM-HRP) (1:300; Jackson ImmunoResearch Laboratories Inc., West Grove, Pa.). After removal of free DAM-HRP, the amplification reagent was added for 4 min, before cell nuclei were stained for 2 min using DAPI (4′,6′-diamidino-2-phenylindole) (D-1306; Molecular Probes, 1.75 ng/ml). Slides were mounted in aquamount (Polysciences, Inc., Warrington, Pa.) and were examined using an Olympus AX70 epifluorescence microscope equipped with motorized stage and Metamorph deconvolution software (Universal Imaging Corporation, Westchester, Pa.). Optical sections were 0.5 μm thick. Composite figures were made using Photoshop (Adobe Systems).

Viral envelope staining with biotinylated CD4-IgG2. As an alternative to staining for viral *gag* protein, DC-associated SIV was also identified using biotinylated tetravalent human CD4-IgG2 (1), which recognizes only the conformationally intact structure of HIV-1/SIV envelope gp120. This reagent was kindly provided by Progenics Pharmaceutical Inc. (Tarrytown, N.Y.). Immunostaining was performed using the FITC-TSA kit with minor modifications to the protocol described above. All reagents were diluted with blocking buffer provided by the TSA kit supplemented with 0.05% saponin. PFA-fixed slides were incubated with chromatography-purified whole human IgG (100 μg/ml; Jackson ImmunoResearch) for 30 min to block nonspecific binding. Thereafter, cells were incubated with 25 μg of biotinylated CD4-IgG2 or biotinylated human IgG (Jackson ImmunoResearch) per ml for 30 min followed by a further 30 min of incubation with HRP-conjugated streptavidin (1:100, provided in the TSA kit) before the amplification reagent was added. Slides were mounted and examined by epifluorescence microscopy.

Detection of AT-2 SIV and tracer uptake by immunofluorescence microscopy. To evaluate endocytic uptake of FITC-DEX or ALEXA-TF by immature and mature DCs in the presence of AT-2 SIV, aliquots of tracer-loaded AT-2 SIV-pulsed DCs were adhered to glass slides and immunostained for p27 Ag using the MAb KK64 (see above). In order to identify and localize internalized FITC-DEX or ALEXA-TF and virus at the single-cell level, p27-labeled cells were identified using a TSA kit carrying the red fluorophore cyanine 3. Immunofluorescence staining was performed as described above, and slides were mounted and examined by epifluorescence microscopy.

Electron microscopy. DCs were collected, washed in ice-cold cRPMI, and incubated with whole infectious or AT-2-treated SIV particles (3 ng of p27 Ag/10^4 DCs) for different lengths of time at 37°C, washed, and fixed with Karnovsky's formaldehyde-glutaraldehyde fixative. In some experiments cells were incubated with virus for 15 min at 4°C before they were warmed up to 37°C for an additional period of 120 min. At that time, the cells were spun out of serum-containing medium and were immediately fixed with Karnovsky's form-

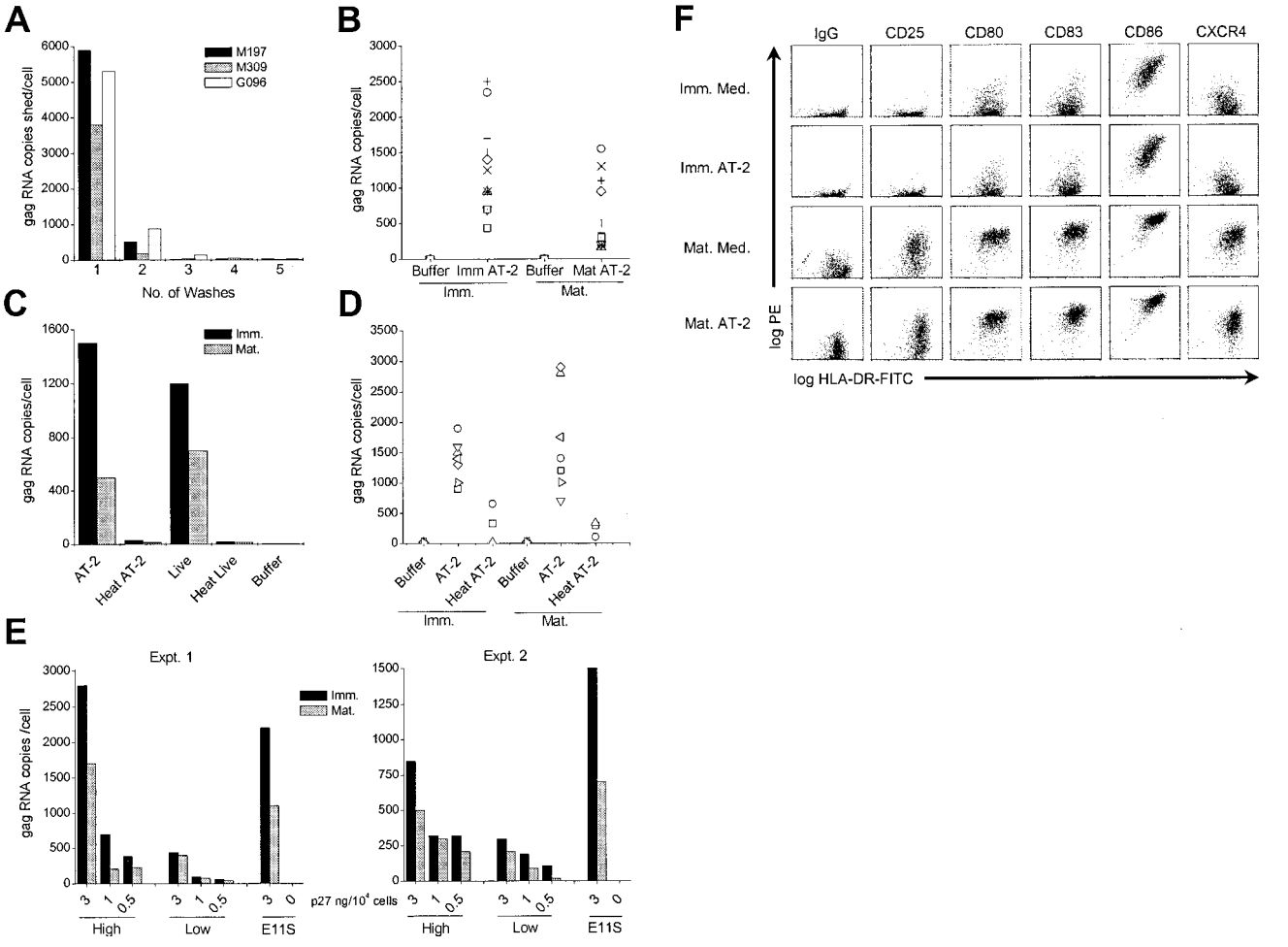

FIG. 1. SIV *gag* RNA is associated with healthy immature and mature DCs. Human (B and C) and macaque (A and D) immature (Imm.) or mature (Mat.) DCs were incubated with 15 to 30 ng of virus p27 Ag/10^5 cells for 2 h at 37°C and washed, and pelleted cells were analyzed for the presence of SIV *gag* RNA by RT-PCR. The *gag* RNA copy numbers per sample were normalized to the numbers of input cells used in each experiment. (A) Aliquots of each of the five washes of AT-2 SIV-pulsed macaque DCs (donors M197, M309, and G096) were collected, and the number of cell-free *gag* RNA copies was ascertained. (B) DCs from 11 different human donors were pulsed with AT-2 SIV (AT-2) or buffer to assess the *gag* RNA levels. Each symbol represents a pair of immature and mature DCs from separate donors. (C) Human DCs were pulsed with AT-2 SIV, heat-treated AT-2 SIV (Heat AT-2), infectious SIV (Live), heat-treated infectious SIV (Heat Live), or buffer and were washed before the *gag* RNA copies were measured. The result of a representative experiment out of five independent experiments is shown. (D) Macaque DCs were exposed to AT-2 SIV, heat-treated AT-2 SIV, or buffer. Each symbol reflects the *gag* RNA levels for three to eight distinct donor pairs of immature and mature DCs. (E) Human immature and mature DCs were incubated with 3, 1, and 0.5 ng of AT-2 SIVmac239 versus SIVmac239/251 p27 Ag per 10^4 cells for 2 h at 37°C and were analyzed for the presence of SIV *gag* RNA. The results of two independent experiments are shown. (F) Human immature and mature DCs exposed to AT-2 SIV or buffer were fluoresecently double labeled with FITC-conjugated anti-HLA-DR (*x* axes) and PE-conjugated anti-IgG, -CD25, -CD80, -CD83, or -CD86 (*y* axes) and were examined by flow cytometry.

aldehyde-glutaraldehyde fixative. All specimens were postfixed in osmium tetroxide and contrasted with 0.5% veronal-buffered uranyl acetate. In some cases cells were not washed after Karnovsky's formaldehyde-glutaraldehyde fixation but were immediately reacted with cationized ferritin (final concentration, 0.32 mg/ml; Bio-Yeda, Rehovot, Israel). Samples were then dehydrated and embedded in Epon 812 resin. Ultrathin sections were mounted on nickel grids, contrasted with lead citrate and were examined in the transmission electron microscope (Phillips EM 400; Fei Company Electron Optics, Eindhoven, The Netherlands). Statistical analysis was performed with Student's *t* test for paired samples.

RESULTS

Association of AT-2 SIV with immature and mature DCs revealed by RT-PCR analysis. To investigate whether whole inactivated noninfectious AT-2 SIV can be captured by immature or mature human and macaque DCs, cells were exposed to virus for 2 h at 37°C and the amount of DC-associated virus was quantified by detecting SIV *gag* RNA copies by real-time RT-PCR analysis. To ensure quantitation of cell-associated virus, virus-pulsed DCs were washed five times and samples of each wash were collected and analyzed for viral *gag* RNA copies. As shown in Fig. 1A, the bulk of unbound AT-2 SIV was removed in the first wash, while remaining virions were cleared with the second wash. Washes 3 to 5 were virtually negative for viral *gag* RNA. Similar results were obtained by enzyme-linked immunosorbent assay monitoring of the viral *gag* protein p27 (data not shown). Thus, cell-free virus is efficiently removed under these washing conditions and the SIV

TABLE 1. SIV *gag* RNA copy numbers captured by immature and mature DCs[a]

Cell source	Results for:			
	Immature DCs		Mature DCs	
	% Of input	RNA copies/cell	% Of input	RNA copies/cell
Human	34	1,312	14	621
Macaque	31	1,341	38	1,678

[a] The *gag* RNA copies/cell were determined by RT-PCR and the percentage of input virus was calculated accordingly. The means of the data displayed in Fig. 1 for the 11 human and 8 macaque immature or mature DC pairs are shown.

gag RNA copies detected in pelleted cell fractions of virus-pulsed DCs (below) likely represent DC-associated virions.

Using this approach, we found that immature and mature human as well as macaque DCs efficiently captured AT-2 SIV (Fig. 1B to E and Table 1). Donor-dependent variations in the total amount of DC-associated virus were observed for both human and macaque DCs. The copy numbers of SIV *gag* RNA per human DC (from 11 donors) ranged from 160 to 2,350 copies per cell (Fig. 1B; Table 1). Immature human DCs captured approximately twice the virus that mature DCs did, except for 1 of the 11 donors shown (indicated with the × symbol). On average, immature human DCs captured 34% (7.2 to 83%) of the input virus, while mature DCs captured 14% (3.5 to 36%) (Table 1). The difference between immature and mature human DCs in the amount of captured SIV is statistically significant ($P < 0.0001$). These observations were also true for DCs exposed to matched infectious SIV (Fig. 1C), suggesting that the association of AT-2 SIV and infectious SIV with immature and mature DCs was comparable. In marked contrast, the amount of viral RNA associated with DCs was dramatically decreased when the DCs were exposed to AT-2-treated or infectious SIV subjected to heat treatment (56°C for 1 h) prior to incubation with target cells (Fig. 1C). Heat treatment has been shown previously to abrogate CD4-dependent binding and cell fusion capability of AT-2-treated virus (45), while such heat treatment has also been shown recently to facilitate dissociation of gp120 from virions (E. N. Chertova et al., unpublished data). These observations suggest that association of SIV with DCs is likely dependent on the integrity of heat-labile viral envelope glycoprotein complexes on the virion surface. Immature and mature macaque DCs captured comparable levels of viral *gag* RNA, ranging from 700 to 2,900 RNA copies per cell as calculated for eight donors (Fig. 1D and Table 1), representing averages of 31 and 38% of the input virus, respectively (Table 1). As with human DCs, heat treatment of AT-2 SIV dramatically decreased the ability of virions to associate with macaque DCs (Fig. 1D). Thus, both immature and mature primate DCs readily capture AT-2 SIV in a manner that appears to require functional Env glycoproteins on the virus surface.

To further evaluate the role of functional viral Env proteins in the association of SIV with DCs, we performed comparative studies using AT-2-treated virions produced from the wild-type clone SIVmac239 and the molecular engineered clone SIVmac239/251 tail. The modified SIVmac239/251 tail clone carries about 10 times the amount of gp120 on its surface that the wild-type virus does (Chertova et al., unpublished). Human immature and mature DCs were pulsed with titrated amounts of SIVmac239 or SIVmac239/251 tail and were compared to SIVmneE11S at the highest dose (3 ng of p27 Ag/10^4 cells). The gp120 content of SIVmneE11S virions is comparable to that of SIVmac239/251 tail virions, approximately 10-fold more than that of wild-type SIVmac239 virions (Chertova et al., unpublished). Figure 1E shows the results of two independent experiments. Comparable amounts of SIVmneE11S and the SIVmac239/251 clone were readily captured by immature and mature DCs. In contrast, following incubation with comparable amounts (based on $p27^{gag}$ content) of SIVmac239, which has approximately 10-fold less gp120 content than does SIVmac239/251 tail or SIVmneE11S, the same cells captured two- to sixfold less virus. The Env dependence of the association of SIV with DCs was further emphasized by the titration effect of both SIVmac239 and SIVmac239/251 clones on immature and mature DCs.

While considerable amounts of virus were captured by the DCs, this did not have any demonstrable effect on the phenotypic characteristics of the cells (Fig. 1F), as assessed by flow cytometry. The phenotype was analyzed immediately after DCs were exposed to virus for 2 h (Fig. 1F) and after culture of virus-pulsed DCs for 24 or 48 h (data not shown). Figure 1F shows a representative experiment (of six independent experiments), demonstrating that exposure of cells to AT-2 SIV neither led to maturation of DCs nor induced a reversion of the mature DC to a more immature phenotype. Phenotypic stability of immature and mature DCs was equally apparent after 24 and 48 h. The same observation was made when infectious virus was used (data not shown). As expected (37), immature DCs exhibited moderate HLA-DR and CD86 expression and low levels of CD25, CD80, CD83, CCR5, and CXCR4. Mature DCs up-regulated all of these markers at least 10-fold (Fig. 1E), except for CCR5, which was down-regulated during maturation to undectectable levels (data not shown). The presence of significant amounts of virus being associated with the cells also had no impact on the T-cell-stimulatory capacity of immature or mature DCs, as determined in a mixed-lymphocyte reaction (data not shown). The percentage yield of viable immature or mature DCs after virus (AT-2 or live SIV) exposure was almost identical to the numbers obtained from cells kept in medium only. Thus, DCs that had entrapped significant amounts of virus exhibited a stable phenotype and their viability and T-cell-stimulatory capacity were unaffected.

AT-2 SIV-loaded DCs carry functionally intact viral envelope protein. The RT-PCR data described above suggested that association of AT-2 or infectious SIV with DCs requires functional envelope gp120. To investigate whether the conformational and functional integrity of the SIV envelope is also preserved after association of the virus with DCs, we tested the ability of DC-associated AT-2 SIV to mediate cell-cell fusion.

Virus-pulsed DCs (2 h at 37°C) were washed and cocultured with the SIV-susceptible and fusion-competent cell line CEMx174 for 2 h at 37°C. Formation of syncytia in the cultures was initially visualized using a light microscope and was evident within 1 h. After 2 h of coculture, the numbers of syncytia were then quantified on Giemsa-stained cytospins where syncytia were identified as MGCs containing more than two nuclei. As summarized in Fig. 2A, AT-2 SIV-exposed immature and mature DCs mediated cell fusion to similar extents. This was comparable to the levels induced by DCs bearing matched

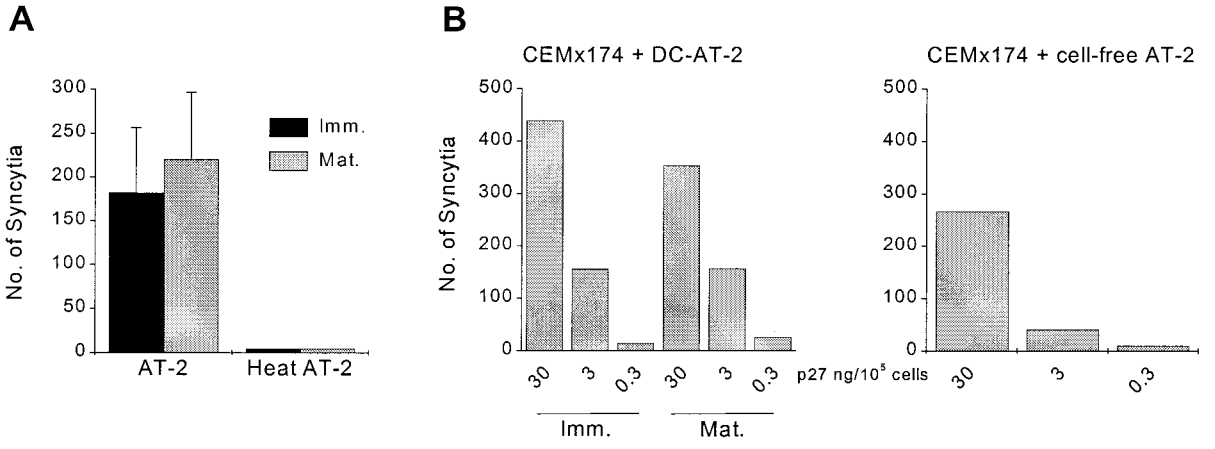

FIG. 2. DC-captured AT-2 SIV retains its fusogenic capacity. (A) Immature and mature human DCs were exposed to 30 ng of AT-2 SIV p27 Ag versus heat-treated AT-2 SIV per 10^5 cells (2 h at 37°C), washed, and cocultured with untreated CEMx174 cells at a DC-to-CEMx174 cell ratio of 1:10. After 2 h at 37°C, cytospins were prepared and the numbers of syncytia per cytospin were counted. The mean numbers of syncytia (± standard deviation) per slide from six independent experiments are shown. (B) DCs were incubated in the presence of AT-2 SIV at 30, 3, or 0.3 ng of p27 Ag/10^5 cells and washed, and 10^4 virus-loaded DCs were cocultured with 10^5 CEMx174 cells for 2 h at 37°C (CEMx174 + DC-AT-2). Alongside, cell-free AT-2 SIV was added at 30, 3, or 0.3 ng of p27 Ag per 10^5 CEMx174 cells (CEMx174 + cell-free AT-2). The numbers of syncytia were determined as described for panel A. Results of one representative experiment out of two are shown.

infectious SIV (data not shown). As expected, MGC formation did not occur when DCs pulsed with heat-treated AT-2 SIV were cocultured with CEMx174 cells or when the heat-treated virus was directly added to CEMx174 cells even at high amounts (data not shown). DCs loaded with AT-2 SIV and cultured in the absence of CEMx174 cells did not form syncytia during this period (data not shown). Similar observations were made for human (Fig. 2) and macaque (data not shown) DCs.

Although RT-PCR data (Fig. 1A) indicated that most cell-free AT-2 SIV was removed by the washing procedure, formation of MGCs revealed in Fig. 2A could have been mediated by low levels of cell-free AT-2 SIV present in the virus-pulsed DC preparations. To further rule this out, we compared the efficiencies of syncytium formation by CEMx174 cells that were cocultured with either DC-bound or cell-free AT-2 SIV (Fig. 2B). Thus, DCs were pulsed with 30, 3, or 0.3 ng of AT-2 SIV p27 Ag per 10^5 DCs for 2 h at 37°C and washed, and 10^4 virus-pulsed DCs were mixed with 10^5 untreated CEMx174 cells and cocultured for 2 h at 37°C before syncytia were counted. Alongside, CEMx174 cells were mixed with the same amounts of cell-free AT-2 SIV p27 Ag per 10^5 CEMx174 cells and syncytia were counted after 2 h of culture. Figure 2B highlights how in cocultures of AT-2 SIV-loaded DCs and CEMx174 cells, more MGCs were detected than in cultures where even higher levels of cell-free AT-2 SIV were added to CEMx174 cells. Namely, based on the input amount of p27 Ag and assuming that 14 to 34% of this virus was entrapped by human DCs (Table 1), then approximately 30- to 70-fold less virus was added in the cell-associated form to the CEMx174 cells. These results indicate that after immature or mature DCs have trapped AT-2 SIV, the functional integrity of the viral envelope is retained and reflected by its fusogenic capacity and also that DC-associated SIV efficiently induces cell-cell fusion, compared to cell-free virus.

Comparable binding of AT-2 SIV to immature and mature DCs. Our initial studies revealed that within 2 h at 37°C, significant amounts of AT-2-treated or infectious SIV associate with immature and mature DCs. To better appreciate the DC-virus interactions, we next studied the kinetics of binding of AT-2 SIV to DCs at 4°C. Initially immature and mature DCs were exposed to virus for 5, 15, 30, 60, and 120 min on ice and washed, and the amount of DC-bound virus was quantified by RT-PCR (Fig. 3A). The presence of virus was also monitored by immunostaining for viral envelope gp120 (Fig. 3B), as well as by the cell fusion assay (data not shown).

RT-PCR analysis revealed that AT-2 SIV binding to both immature and mature DCs occurred within 5 min and gradually increased over time (Fig. 3A). The amount of AT-2 SIV that bound to immature and mature DCs was similar, but the levels of DC-associated virus captured during 2 h at 4°C were slightly lower than those detected after 2 h at 37°C (compare Fig. 1 and 3A). Little if any viral RNA was detected in DCs exposed to heat-treated virus (data not shown). These data further support our initial observations that the DC-virus interaction is dependent upon the presence of functional molecules on the virus surface. Using our cell fusion assay, we confirmed that AT-2 SIV bound to the DCs is fusion competent, much like virus that associated with DCs at 37°C (data not shown).

Immunofluorescence microscopy was then used to follow virus binding to DCs at the single-cell level. As described above, immature and mature DCs were exposed to AT-2-treated or infectious SIV at 4°C and were washed before cells were adhered to alcian blue-coated glass slides. To further enhance the Ag-specific staining signal of DC-bound virus, biotinylated CD4-IgG2 was used to visualize gp120. Signal amplification of gp120-stained cells was achieved using the FITC-conjugated TSA kit. Immunostaining for the viral envelope protein confirmed distinct virus binding to the cell membranes of immature and mature DCs (Fig. 3B). In agreement with the RT-PCR data, the intensity of SIV envelope staining on immature and mature DCs increased with time (data not shown). Similar binding was detected when live SIV was used (data not shown). Essentially the same was observed when DCs

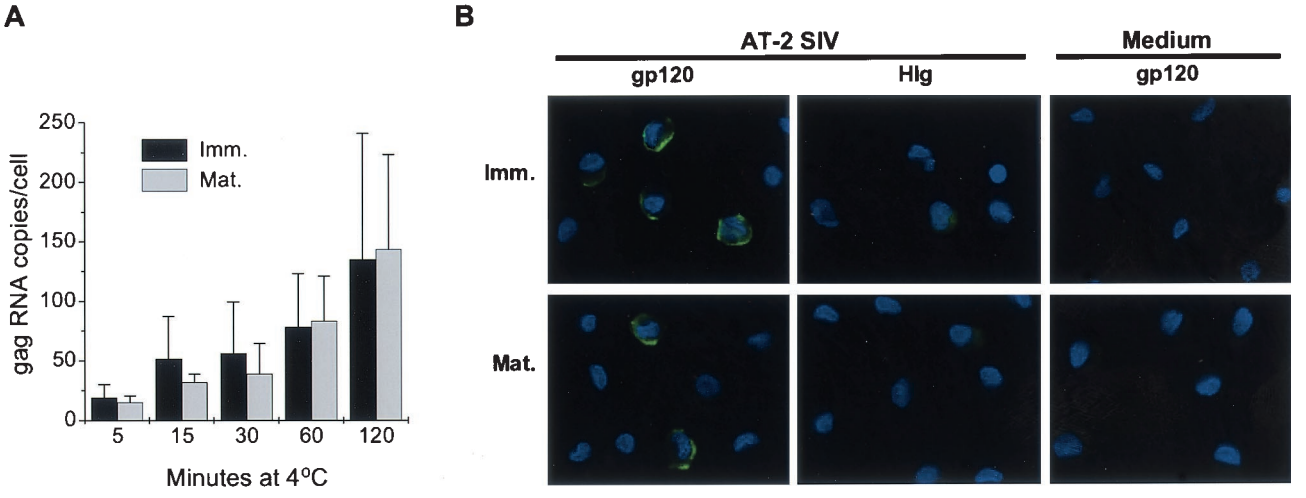

FIG. 3. AT-2 SIV binds comparably to immature (Imm.) and mature (Mat.) DCs. Human immature and mature DCs were incubated with AT-2 SIV (15 ng of AT-2 SIV p27 Ag per 10^5 cells) for the indicated times at 4°C. At each time point, the cells were washed and pelleted for RT-PCR analysis (A) or aliquots were taken for fluorescence microscopy (B). (A) RT-PCR analysis was performed to determine the numbers of DC-associated virus at 4°C. The mean numbers of RNA copies per cell (± standard deviation) of two independent experiments are shown. (B) DCs exposed to AT-2 SIV (versus medium) for 120 min at 4°C were collected, adhered to alcian blue-pretreated slides, and fixed with 4% PFA. Saponin-treated cells were immunofluorescently labeled for SIV envelope gp120 using CD4-IgG2 (in green), and nuclei were stained with DAPI (in blue). The staining for envelope protein was compared to the human IgG (HIg) control on AT-2 SIV-pulsed DCs as well as to the CD4-IgG2 staining of medium-pulsed DCs. Magnification, ×100.

were stained for the *gag* p27 Ag; however, the intensity of staining was weaker than the envelope staining (data not shown). Negligible background staining was observed on pulsed DCs stained with the biotinylated human IgG control or on buffer-treated cells stained with biotinylated CD4-IgG2. These results illustrate how AT-2-treated or infectious SIV bind similarly to both immature and mature DCs.

AT-2 SIV is efficiently captured and taken up by DCs at 37°C. As indicated by RT-PCR (Fig. 1) and immunofluorescence microscopy (Fig. 3), AT-2-treated or infectious SIV was bound by both immature and mature DCs in a similar manner, yet the initial assessment of DC-virus association suggested that the process of virus capture by DCs was more efficient at 37°C. Therefore, we looked more closely at the kinetics of virus association with DCs at 37°C and the fate of virus captured by the cells. After DCs were exposed to AT-2 SIV for 5, 15, 30, 60, and 120 min at 37°C, including the donors used for the binding study (above), the amount of DC-associated virus was quantified by RT-PCR analysis (Fig. 4A). As shown in Fig. 4A, after the initial association of AT-2 SIV with DCs within the first 5 min, a steady increase in the amount of DC-associated virus was observed, which peaked between 60 and 120 min. These viral RNA levels were consistently greater than those seen at 4°C (Fig. 3). The approximately 2.5-fold-stronger signal for viral *gag* RNA with immature human DCs (Fig. 1B and C and Table 1) was apparent at each time point examined (Fig. 4A).

To visualize the fate of virus taken up by the immature and mature macaque (Fig. 4B) or human (Fig. 4C) DCs, confocal microscopy was used. DCs were pulsed with either AT-2 or infectious SIV for 5 to 120 min at 37°C and were immunofluorescently labeled for the viral Gag protein p27 or the envelope gp120. During the first 15 min at 37°C, SIV staining was evident at the periphery of both immature and mature DCs, much like the pattern of gp120 staining seen at 4°C (data not shown). To our surprise, the localization of p27 and gp120 dramatically changed in mature DCs when exposed to virus for longer than 15 min at 37°C. Examination of mature DCs between 30 and 120 min at 37°C revealed that both p27 and gp120 moved into distinct intracellular vesicular locations, often concentrated as one spot that was sometimes found deep inside the cell close to the nucleus. In contrast, in immature DCs the Gag or envelope staining consistently remained mainly at the periphery closely associated with the plasma membrane. These distinctions are highlighted in Fig. 4 (120 min). Identical staining patterns were also obtained when the SIVmac239 or SIVmac239/251 clones were used (data not shown), with the SIVmac239/251 showing stronger staining than the SIVmac239, in agreement with the RT-PCR data (Fig. 1E). Independent of whether cells were stained with the anti-p27 MAb or biotinylated CD4-IgG2, the same pattern was observed (Fig. 4C). Essentially equivalent results were also found when infectious SIVmneE11S was used, underscoring the similarities in how AT-2-treated and infectious SIV are handled by DCs. This distinction in protein staining of immature versus mature DCs was true for macaque (Fig. 4B) and human (Fig. 4C) DCs. Together these data confirm that mature DCs are able to efficiently internalize whole virions and show that the location of internalized virion-derived proteins is dramatically different in immature and mature DCs.

Internalized SIV localizes into large intracellular vesicles in mature DCs. To further address the cellular location of the virus versus viral protein in immature and mature DCs in more detail and to investigate whether DCs are able to take up whole virions, electron microscopy studies were performed. Human or macaque immature and mature DCs were exposed to virus, washed, and immediately fixed before being processed for electron microscopy. As illustrated in Fig. 5 whole, structurally intact virions were taken up by immature and mature

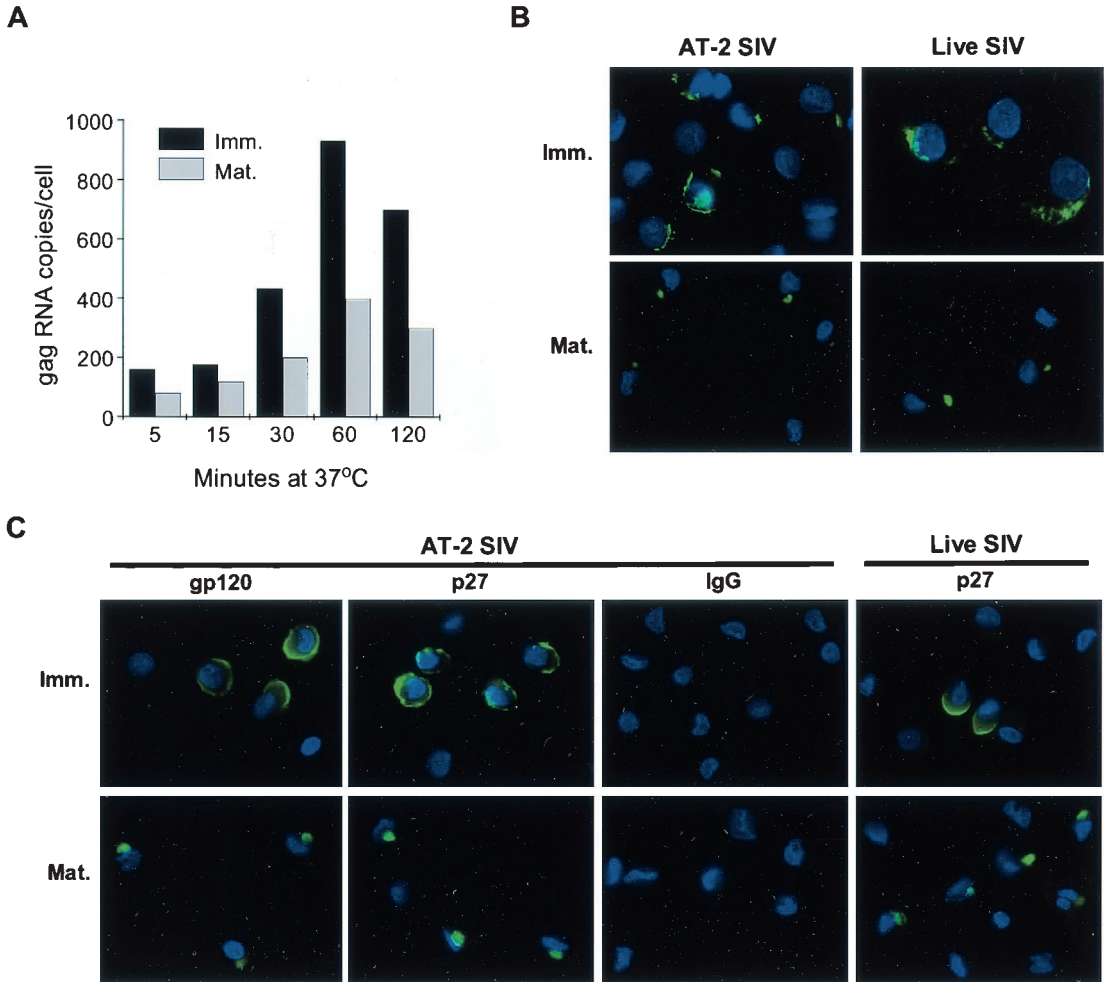

FIG. 4. AT-2 SIV ingested by immature (Imm.) and mature (Mat.) DCs targets to different intracellular locations. Human (A and C) and macaque (B) immature and mature DCs were exposed to AT-2 or live SIV (15 ng of SIV p27 Ag/10^5 cells) at 37°C before being processed for RT-PCR analysis (A) and immunostaining (B and C). (A) Washed, AT-2 SIV-pulsed DCs were collected at the indicated time points, and the numbers of SIV *gag* RNA copies were determined. Results of one representative experiment out of four comparable experiments are shown. Macaque (B) or human (C) DCs exposed to AT-2 or live SIV for 120 min at 37°C were immunostained for envelope gp120 (C) or p27 Ag (B and C) versus IgG (in green). DAPI-stained nuclei are in blue. Controls of human Ig staining of pulsed DCs and envelope staining of unpulsed DCs were negative as shown in Fig. 3. Data shown are representative of four to six comparable experiments. Magnification, ×100.

DCs. Somewhat to our initial surprise, considerably more whole, intact virus particles were apparent in electron micrographs of mature DCs (Fig. 5A to D, G, and H). In contrast, virus-pulsed, immature DCs showed considerably fewer internalized virus particles (Fig. 5E and F) but had comparable or greater levels of viral RNA detected by RT-PCR (Fig. 1, 3, and 4). To distinguish virus in true intracellular versus peripheral locations in between veils or other dendritic processes, cells were labeled with the nonspecific cell surface marker cationized ferritin, which binds to anionic sites on the cell surface but is not able to penetrate through the surface membrane (44). Ferrritin-negative vacuoles and virions are regarded as truly internalized. As illustrated in Fig. 5C and D, most compartments containing whole virions that appeared intracellular were ferritin negative and were indeed inside the mature DCs.

The comparison of human immature and mature DCs was investigated in six independent experiments and revealed an average of 14% of immature DCs on a given ultrathin section that contained SIV. In contrast, 41% of all human mature DCs showed internalized virus. The difference between the numbers of virus-carrying immature and mature DCs was statistically significant ($P < 0.05$). Furthermore, the intracellular vesicles in immature DCs contained one or two virions that generally accumulated at the periphery close to the cell membrane (Fig. 5E and F). In dramatic contrast, in mature DCs the internalized virus was localized in large phagocytic vacuoles that also sometimes contained other material morphologically consistent with cell debris or cell membrane microvesicles, which are an inevitable contaminant of even sucrose-banded, highly purified retrovirus preparations (7). Between 15 and 60 cell profiles were analyzed for each condition. In one experiment, virtually every second cell possessed several large, virus-filled vacuoles. In another experiment, 7 of 15 cells contained six to nine large vacuoles harboring virus. In separate experiments we compared the uptake of the AT-2-treated SIV to that of the unmodified, infectious SIV. In all three experiments, the

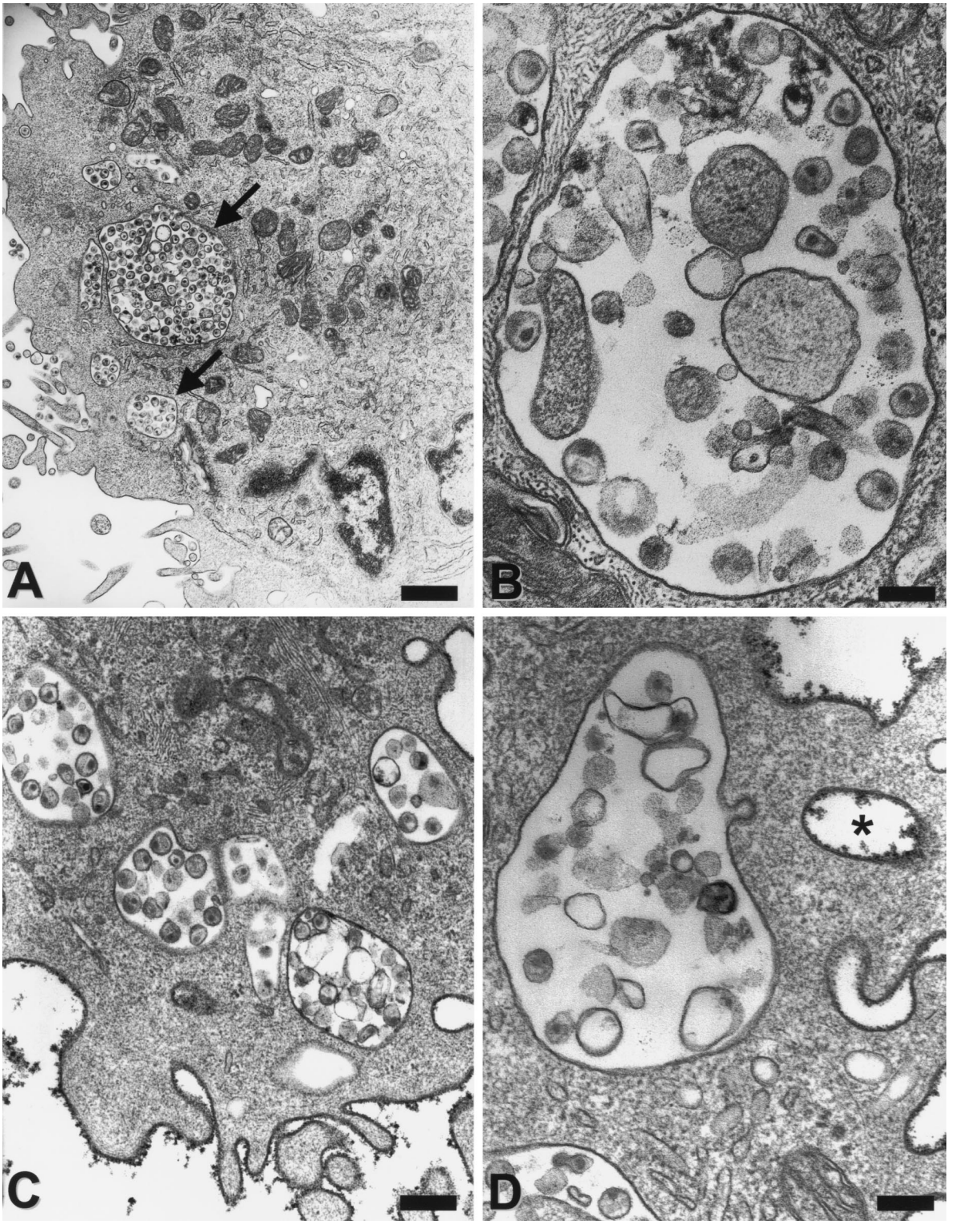

FIG. 5. Uptake of AT-2-treated and live SIV into human and macaque DCs. After immature and mature human (A, B, and E to H) and mature macaque (C and D) DCs were incubated with AT-2 (A to F) or live SIV (G and H) (30 ng of p27 Ag/10^5 cells) for 2 h at 37°C, cells were immediately fixed and processed for electron microscopy. Note the large phagocytic vacuoles containing many virus particles (some arrowed) in mature human and simian DCs (A to D). For panels C and D, cationized ferritin (dark, granular deposits) was used to distinguish true intracellular vacuoles from vacuoles that are open to the extracellular space. Virus in ferritin-negative organelles only represents endocytosed virus. For comparison, a seemingly intracellular vesicle may be recognized as extracellular by its ferritin label (asterisk). Immature DCs (E and F) take up fewer virus particles that are mostly localized close to the surface membrane (arrows). Live SIV (G and H) is endocytosed by mature DCs similar to AT-2-treated virus. Note an area of active uptake at the upper pole of the cell in panel G, which likely coincides with polarized protein staining that was sometimes observed (Fig. 4). Magnifications and scale bars: ×8,400/1.2 μm (A and G); ×51,000/200 nm (B and D); ×30,000/300 nm (C and E); ×21,000/500 nm (H); and ×72,000/140 nm (F).

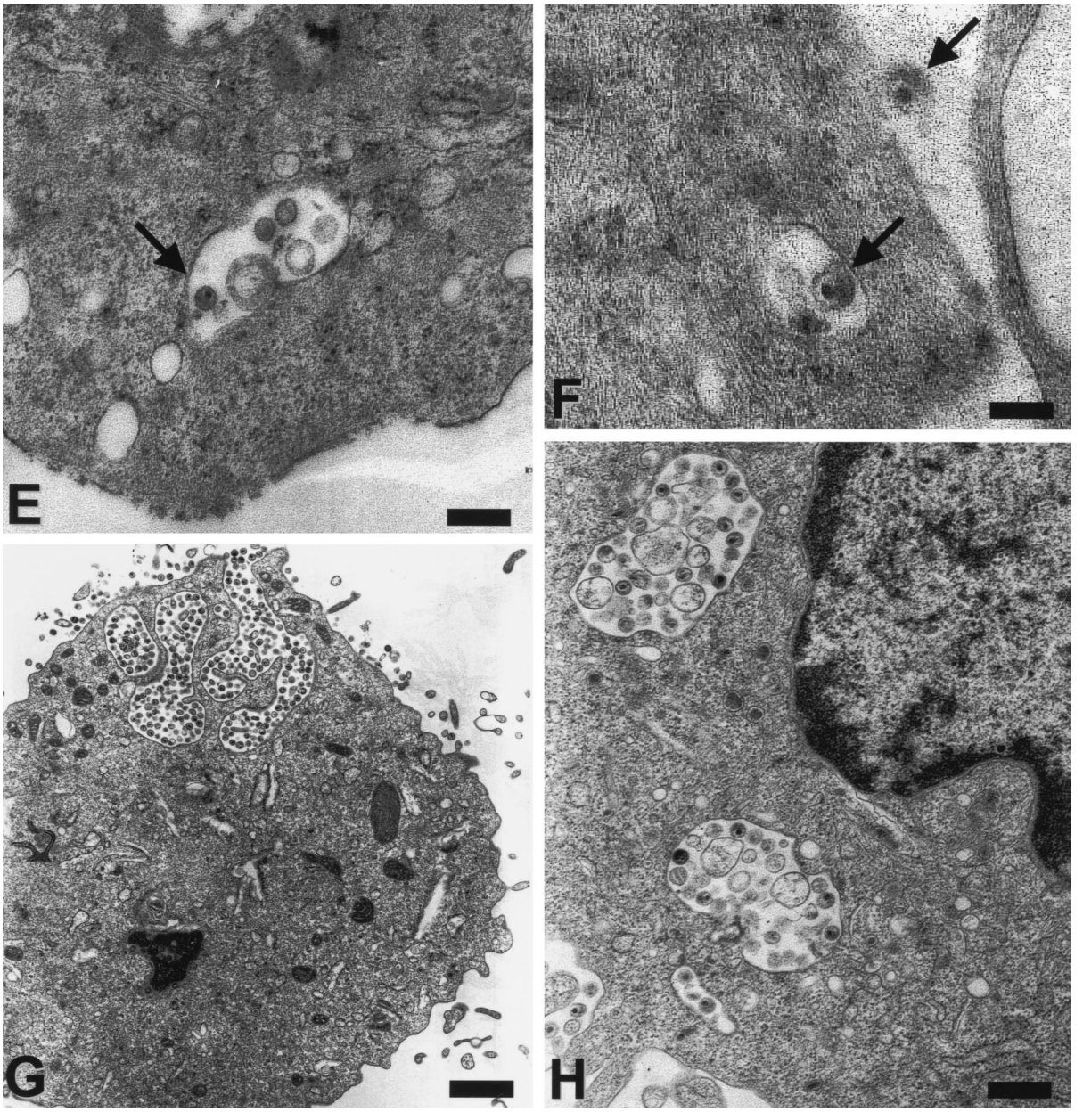

FIG. 5—*Continued.*

live SIV behaved like the AT-2 SIV (Fig. 5G and H). Basically the same observations were made with monkey DCs (Fig. 5C and D). Although the quantitative differences in the uptake of virus between immature and mature macaque DCs was less strongly pronounced (Fig. 1 and Table 1), the pattern of virus uptake was consistent for all human and monkey cells. Large vesicles containing numerous virions were found only in mature DCs (Fig. 5C and D), while the few single virions internalized by immature DCs always remained cell membrane associated. The data shown here demonstrate for the first time in paralleled comparison that mature DCs are more efficient in internalizing structurally intact virus particles than are the highly endocytically active immature DCs. Furthermore, these data also reveal a significant difference in the intracellular fates of internalized virions in immature and in mature DCs.

Live and AT-2 SIV bind to clathrin-coated pits of immature and mature DCs. DC maturation induces a rapid inhibition of endocytosis (3, 15, 28, 37, 46), selectively affecting the nonspecific uptake mediated via macropinocytosis or phagocytosis, while it does not decrease the number of plasma membrane clathrin-coated pits (and vesicles which are indicative for antigen-specific uptake via binding to a receptor molecule expressed on the target cell) (15, 37). To examine whether AT-2 and live SIV can adhere to clathrin-coated pits in immature and mature DCs, electron microscopy analysis was performed. To ensure efficient virus binding, DCs were first incubated with

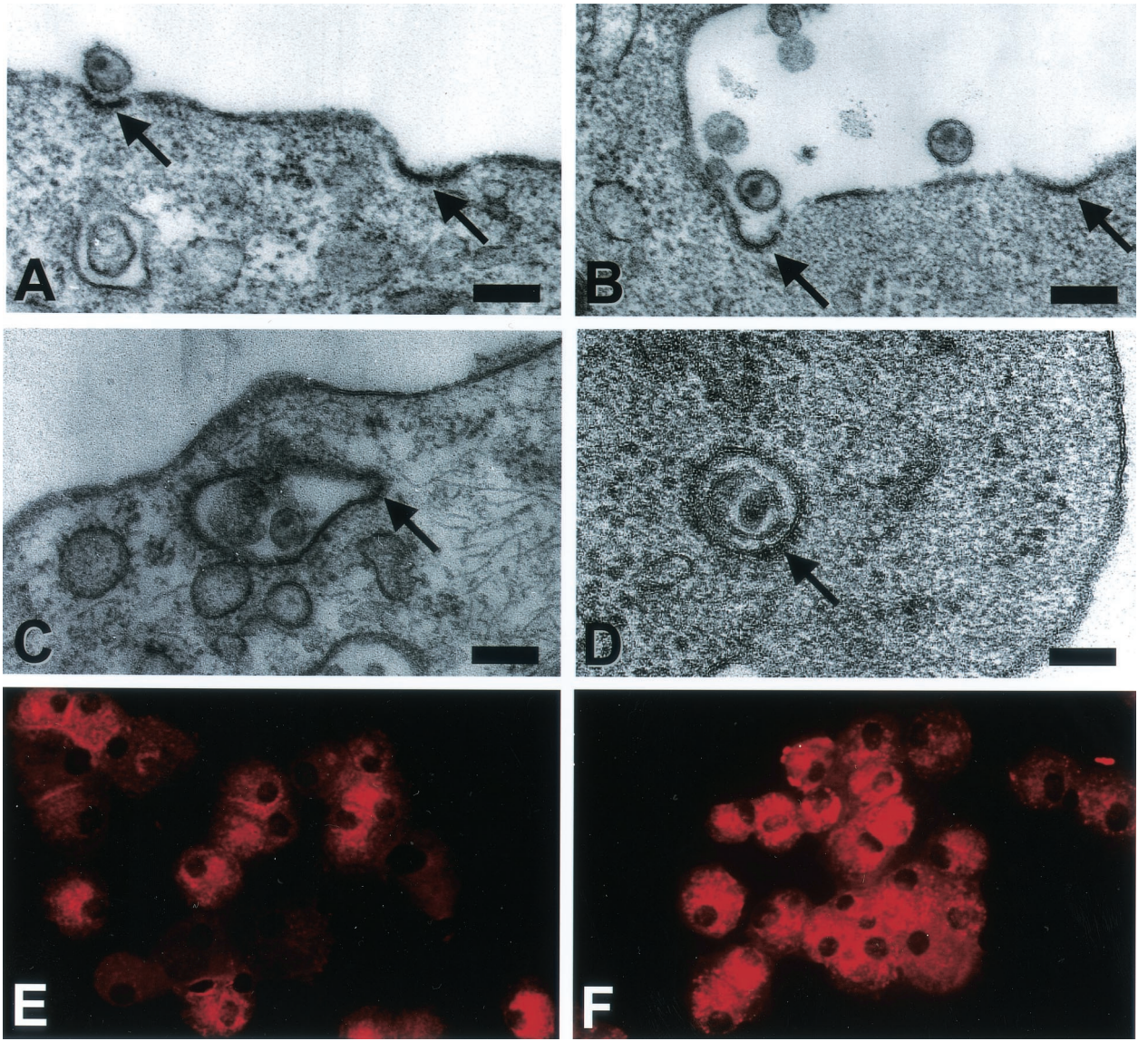

FIG. 6. Virus particles are taken up via clathrin-coated pits by immature and mature DCs. Human immature (A, B, and D) and mature (C) DCs were first incubated for 15 min at 4°C with AT-2 SIV (30 ng of SIV p27 Ag/10^5 cells). After a further 1 min (C), 5 min (A), or 120 min (B and D) at 37°C, the cells were washed, fixed, and processed for electron microscopy. Whole, structurally intact virus can be spotted bound to coated pits (A and B, arrows) and localized in coated vesicles close beneath the plasma membrane surface (C and D, arrows). Magnification and scale bars: ×50,000/200 nm (A); ×41,000/240 nm (B); ×47,000/210 nm (C); and ×80,000/120 nm (D). Cytospin-adhered human immature (E) and mature (F) DCs were fluorescently labeled for clathrin (X-22) and revealed comparable amounts of clathrin-coated structures.

virus (AT-2 or live SIV) for 15 min at 4°C before being warmed up to 37°C for short periods (1, 5, 15, 30, and 120 min), washed, and immediately fixed and processed for electron microscopy. While preincubation of DCs with virus at 4°C led to sufficient virus binding, it did not alter the subcellular fate of internalized virus upon culture at 37°C (data not shown). At 5 min virions were found bound to clathrin-coated pits and some virions were already localized in coated vesicles just beneath the cell surface membrane (Fig. 6). While single virus-containing vesicles stayed close to the plasma membrane over the 120-min incubation in immature DCs, these structures were mainly detected within the first 30 min in mature DCs (data not shown).

To further demonstrate that the cocktail-induced maturation of DCs did not affect clathrin structures, DCs were immunolabeled for clathrin. Figure 6 shows no gross differences in the clathrin expression by immature (Fig. 6E) or mature (Fig. 6F) DCs, confirming previous observations (15, 37). The results from these experiments clearly show that SIV binds and also can be taken up by clathrin-coated pits by immature as well as mature DCs, indicating the involvement of a receptor-mediated uptake mechanism of SIV by DCs of divergent differentiation stages.

AT-2 SIV-exposed DCs exhibit normal endocytic function. Having demonstrated that virus can bind to and be internalized by clathrin-coated pits in immature and mature DCs, we next ensured that the presence of virus did not alter the endocytic

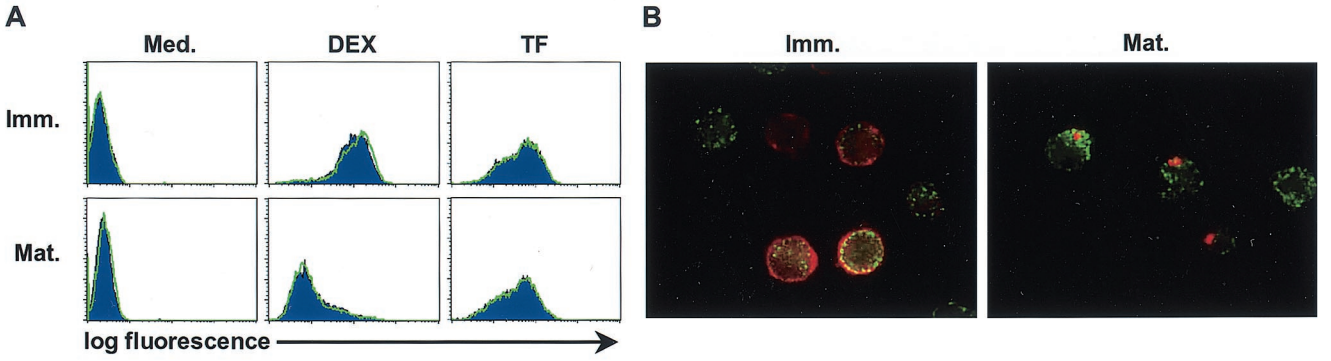

FIG. 7. Uptake of AT-2 SIV by DCs does not alter DC endocytic functions. Immature (Imm.) and mature (Mat.) human DCs pulsed with AT-2 SIV (15 ng of p27 Ag/10^5 cells) or buffer for 60 min at 37°C were exposed to FITC-DEX (DEX) or ALEXA-TF (TF) or medium (Med.) for the last 30 min. (A) Buffer- (filled histograms) and AT-2 SIV-treated (lines) DCs that were incubated with medium (Med.), DEX, or TF underwent FACS analysis to monitor tracer uptake (green fluorescence intensity [log fluorescence] is revealed on the *x* axes). (B) Aliquots of TF-loaded (green), AT-2 SIV-pulsed, immature and mature DCs cells were adhered to alcian blue-pretreated slides and fixed with 4% PFA, and saponin-treated cells were immunofluorescently labeled for p27 Ag (red). Representative results of one experiment out of five comparable experiments are illustrated. Magnification, ×100.

function in particular of mature DCs. Distinct forms of endocytosis were monitored by using fluorescently labeled tracers, including FITC-DEX, Lucifer Yellow (LY), and ALEXA-TF. While DEX is predominantly taken up via the macropinocytic pathway with some contribution from the macrophage mannose receptor (MMR, CD206), LY is described as being exclusively taken up by macropinocytosis (46). In contrast, internalization of TF is mainly TF receptor (CD71) mediated. As shown in a representative experiment depicted in Fig. 7A, the uptake of DEX or TF was unaltered in AT-2 SIV-loaded DCs compared to in medium-treated DCs. In five independent experiments, immature DCs exposed or not exposed to AT-2 SIV actively ingested DEX and TF, while in mature DCs the macropinocytic uptake of DEX was drastically diminished. The uptake of LY was also down-regulated to the same amount in mature DCs with or without virus treatment, mimicking DEX uptake (data not shown). In contrast, the amount of accumulated TF remained constant between immature and mature DCs, independent of the presence or absence of virus (Fig. 7A). These data demonstrate that pulsing the cells with AT-2 SIV had no effect on the fluid phase uptake of immature or mature DCs, revealing that the down-modulation by macropinocytic function in mature DCs cannot be reversed by AT-2 SIV. Thus, the presence of AT-2 SIV neither blocked nor enhanced nonspecific uptake of DEX or TF in immature or mature DCs.

Confocal microscopy was used to confirm at the single-cell level that AT-2 SIV and tracers were taken up by the same cells, as well as to evaluate the intracellular location of the virus in more detail. Although unlikely, considering the high numbers of cells entrapping virions (see above), it was possible that the cells taking up AT-2 SIV were not the cells that incorporated the tracers (Fig. 7A) and that AT-2 SIV interfered with tracer uptake in a selected subset of cells. DEX (not shown) or TF uptake (Fig. 7B) was comparable in SIV p27-positive cells as well as in those cells not carrying detectable SIV, further indicating that internalization of AT-2 SIV did not alter the uptake of the various tracers. Immature DCs accumulated DEX in large intracellular structures resembling macropinosomes, while the intracellular p27 protein was located in very distinct structures close to the cell membrane. In mature DCs the macropinocytosis-like structures containing DEX were dramatically decreased and were not overlapping with the perinuclearly situated p27-containing vesicles (data not shown). The amounts of vesicular structures containing accumulated TF were comparable between immature and mature DCs as well, but again, the localization of TF and p27 protein was distinct (Fig. 7B). Together, these data indicate that AT-2 SIV was internalized by mature DCs in which the fluid phase uptake has been down-regulated into cellular locations distinct from those containing macropinocytically ingested DEX or receptor-internalized TF.

DISCUSSION

DCs occupy a central but dichotomous position in the biology of the immunodeficiency viruses. While immature DCs are susceptible to low-level productive infection with R5 HIV-1 strains, viral replication cannot be achieved in mature DCs. But immature and mature DCs are able to trap and then transmit both X4 and R5 HIV-1 strains to T cells which significantly amplify the infection in this process (27). These features likely make DCs a key player in the initial transmission and establishment of HIV-1 in new hosts and also in the overall process of controlling viral replication. On the other hand, DCs are also central in the development of antiviral immune responses through their function as the most potent APCs in the body. As is the case for many viruses, it appears that HIV has coopted normal immune defense mechanisms, subverting them to facilitate the establishment and persistence of infection (10, 40). In relation to DCs, accumulating data suggest that HIV-1 exploits the physiology of this unique cell population with properties that change during differentiation and maturation in a manner that facilitates their function as a critical regulator of immune function. It has been proposed that HIV-1 and SIV take advantage of the ability of DCs to take up particulate Ags, their property of migrating from the periphery to lymph nodes following encounters with Ag and

resulting activation, and their close, efficient interactions with T lymphocytes, including $CD4^+$ T cells, as mechanisms to establish and spread infection in the host (27).

To gain more insight into the virus-DC biology at the cellular level at the very early stage of virus-DC interaction in an attempt to better understand the initial events leading to viral dissemination and/or Ag presentation, we studied the interactions of SIV with both immature and matured monocyte-derived DCs from humans and rhesus macaques. We used a noninfectious virus (AT-2 SIV) as a tool and compared it with native infectious SIV, both of them containing functional envelope glycoproteins. Comparative studies covering the first 30 to 120 min of DC-virus interplay demonstrated that all observations obtained with the chemically inactivated SIV were reflective of the interactions of DCs with the infectious SIV. Herein we show for the first time in a side-by-side comparison that both immature and mature primate DCs entrap and internalize virus, likely via receptor-mediated pathways, while the immediate intracellular fate of the virus is dramatically different for the two cell populations. This is independent of the amount virus acquired by immature and mature DCs. Strikingly, the poorly macropinocytic mature DCs sequester significantly more whole, structurally intact virions into large vesicles deep within the cells, whereas the endocytically active immature DCs not only retain fewer internalized virions but are also located close to the cell periphery.

Initial analyses confirmed that immature and mature primate DCs captured considerable amounts of fusogenic virus and/or viral proteins (Fig. 1 and 2; Table 1) without any apparent impact on the viability, phenotype, or functionality of the cells (Fig. 1 and 7). Quantitative RT-PCR analysis indicated that approximately twice as much virus was captured by immature human DCs as by their mature counterparts at a statistically significant level. While the distinct cellular distribution of viral proteins and particles was observed in macaque cells (Fig. 4 and 5), the amounts of RNA captured by immature and mature macaque DCs were not statistically significantly different and the amount of viral RNA associated with each subset was comparable to that for human cells (Fig. 1). Overall, the present estimates of viral RNA genome copy numbers per mature DC are much greater than those previously reported using semiquantitative DNA PCR techniques (41, 43), even when smaller amounts of virus were added (Fig. 1E), supporting the idea that large amounts of virus can be captured by mature DCs but that only a fraction (at best) of this can be subsequently reverse transcribed. The RT-PCR approach used here detects all cell-associated viral genomes, not just those that have undergone reverse transcription. Virus simply "entrapped" by the DCs may of course remain infectious and contribute significantly to virus spread to T cells, even in the absence of productive infection of the entrapping DC.

Our studies also clearly demonstrate that the viral envelope glycoproteins of DC-associated virions retain their fusogenic capacity. Studies to assess whether (i) fusogenic virus/proteins are located at the cell membrane versus being released from within the cell, or (ii) whether the resulting syncytia represent DC–T-cell heterokaryons or T-cell–T-cell fusions are in progress, but in either case these findings have important implications for the transmission of infection to T cells and resulting amplification of viral replication. The results may also be relevant to proposed mechanisms by which DCs can sequester virus in a protected state in which it remains infectious and transmissible over several days (12). In agreement with earlier work studying T cells (2, 45), our data demonstrate the need for one or more functional receptors on the virus surface in order to interact with DCs (Fig. 1), underscoring that DCs do not nonspecifically engulf the particles. Interestingly, the number of internalized virions was significantly higher in mature than in immature DCs and virus that was bound to mature DCs trafficked to a distinct intracellular location compared to immature DCs (Fig. 4 and 5). Most dramatically, large vacuolar compartments that tended to concentrate deeper within the cell containing structurally intact virions were only detected with mature DCs, compared to the peripheral localization of the fewer virions internalized by the immature DCs. Strong intracellular SIV Gag or envelope staining in the mature DCs coincided with the detection by electron microscopy of large vacuoles containing numerous, intact, mature virions. In contrast, the cell membrane-associated pattern of SIV Gag or envelope staining within immature DCs paralleled the presence of small vesicles containing one or two particles as observed by electron microscopy, with very few particles being detected on the cell surface. These observations were true for DCs differentiated with MCM or cocktail. A notable difference was observed only when MCM-matured DCs did not fully differentiate, reaching an intermediate maturation stage which correlated with a mixture of p27 staining at the periphery and perinuclear vesicles (data not shown).

Previous in vitro and in vivo reports suggested that DCs can hold virus in cellular compartments (8, 9, 21). In an in vitro approach virus-exposed immature DCs revealed "encircled" virions by electron microscopy (8), and in an in vivo setting DCs isolated from mucosal tissue of HIV-1-infected individuals carried vacuoles containing numerous virions (21). Since the cells in the latter example were already mature at the stage of analysis, it is hard to know whether they captured the virus as an immature or mature cell. In order to define the differentiation state of DCs enabling the entry of whole virions into DCs, as well as to accurately distinguish between really internalized virions versus virions entrapped by membrane invaginations or ruffles, our study emphasized the very early events of DC-virus interactions in classically immature versus mature DCs. This report demonstrates for the first time in a side-by-side comparison of immature and mature DCs that structurally intact virus can be internalized by both immature and mature DCs into ferritin-negative vesicles. It also provides the first comparative report showing that mature DCs preferentially internalize considerable amounts of whole virus. Most strikingly, the ingested virus was handled very differently in the two populations, as was apparent in its distinct intracellular localization. This was initially unexpected, since immature DCs are known to have greater endocytic capacity than do mature DCs, which down-modulate macropinocytic functions upon maturation (Fig. 7) (3, 15, 28, 37, 46). Despite this down-regulation of macropinocytic uptake, a property that did not appear to be altered by the presence of AT-2 SIV, mature DCs ingested large numbers of virions, suggesting that in mature DCs lacking macropinocytic activity, other mechanisms of ingestion of virus were at work.

Thus, a likely alternative explanation is that virus was taken

up via receptor-mediated pathways that were still functioning in the matured DCs. We and others have shown that mature primate DCs retain the ability to take up molecules via receptor-mediated pathways (Fig. 7) (15, 37). DCs take up particles via a number of receptor-mediated mechanisms, including those involving caveolae (54) and clathrin-coated pits (15, 29). Caveolin 1 (a protein associated with caveolae) and clathrin are expressed by human (Fig. 6 and unpublished observations) and macaque immature and mature DCs, but caveola-mediated uptake does decrease somewhat upon maturation (37). Endocytic uptake of whole HIV-1 and SIV through clathrin-coated pits has been demonstrated in other cell types (20, 39). Herein electron microscopy examination confirmed that a considerable proportion of virus appears to have been taken up by DCs via clathrin-coated pits. This was shown by the rapid removal of virus from the cell surface and by association of virus with clathrin-coated pits, as well as concentration of virions engulfed in clathrin-coated vesicles in both immature and mature DCs (Fig. 6). Such internalized virus may remain as infectious particles rendering DCs a latent reservoir and/or lead to viral integration and early gene expression. The latter has been described for viral proteins detectable in the cytosolic (35) and vesicular fractions of cell lines (13). Moreover, similar or slightly more viral RNA was associated with immature DCs and comparable amounts of viral protein were seen by nonquantitative fluorescence microscopy. Yet, the numbers of intact virions visualized by electron microscopy were significantly greater in mature DCs. This suggests that in immature DCs some of the virus may undergo fusion with the cell and/or vacuolar membranes, with the uncoated virus entering the cytosol, possibly leading to productive infection as seen in other cell systems (35), or being degraded in immature DCs, resulting in fewer intact virions being evident by electron microscopy. The observation that AT-2 or live SIV but not their heat-treated equivalents specifically bound to the surface of DCs provides further evidence for receptor-mediated interactions between DCs and the virus. Association of fewer virions with DCs for virions expressing low levels of gp120, compared to SIV virions containing approximately 10-fold higher amounts of gp120, is further indicative of the role of functional viral envelope in this process (Fig. 1).

The work presented here highlights how $CCR5^{+}$, $CXCR4^{low}$ immature DCs and $CCR5^{low}$, $CXCR4^{high}$ mature DCs both captured virus yet directed internalized virus to different locations. The resistance of DCs from individuals bearing a mutant form of CCR5 to acquire HIV-1 suggested a role for this coreceptor in DC-virus interactions needed for infection of immature DCs (19, 48). Although most SIV isolates use CCR5 (56) to enter the cell, it is down-regulated on mature human and macaque DCs, suggesting that this chemokine receptor may play a limited role in the virus binding and internalization described here. Furthermore, the fact that immature and mature DCs exposed to the CXCR4-using HIV-1 MN strain exhibit the same pattern of virus uptake as seen with SIV (Marie Larsson, personal communication) makes it less likely that CCR5 is the sole molecule involved in the uptake of whole virions. Moreover, CD4 and coreceptor-independent binding of HIV-1 by DCs has been described and distinguished from the infection of these cells (8). Adding to the complexity, recent reports suggest the C-type lectin receptor (CLR) DC-SIGN (CD209) as a critical player in capturing R5 and X4 viruses to promote infection of permissive cells in *trans* (16). While the HIV envelope-binding CD209 is expressed by monocyte-derived DCs (16), the level of expression decreases upon maturation (50, 51). Recent evidence (55) revealed that CD209 appears to play a less important role in binding virus in the macaque system, since anti-macaque CD209 Abs that could block the transmission of infection from macaque CD209 transfectants did not impact the transmission of infection from virus-loaded primary macaque DCs to T cells. Moreover, while many DCs express CD209, the DCs at the body surfaces, Langerhans cells, do not (16, 17). This implies that other molecules must serve to interact with the virus during the early stages following mucosal transmission, if these cells are one of the first leukocytes targeted by the virus (11, 22, 43). Langerin (CD207), another CLR expressed by human (52, 53) and macaque Langerhans cells (unpublished observations), has been implicated in endocytosis and is internalized upon maturation. The CLR CD205 which has been shown to be important for particle uptake by DCs (29, 34) is expressed at higher levels in mature blood (37) and skin-derived primate DCs (unpublished observations). In fact, Turville et al. (51) reported that CD209, the macrophage mannose receptor (CD206), and other as-yet-unidentified CLRs may have important roles in binding HIV-1 envelope by distinct DC subsets at specific stages of differentiation. This emphasizes the existence of complex CD4 and chemokine receptor-dependent and -independent binding of the virus to DCs (21, 36, 50, 51) and the potential synergism between these molecules and CLRs (31).

Altogether, the present observations and the cumulative emerging understanding in the field as a whole suggest that DC-virus interactions are multifaceted and complex, being heavily influenced by the differentiation and activation state of the DC involved and the particular DC subsets being examined. The use of noninfectious virions capable of interacting authentically with target cell receptors provides a unique approach for studying the earliest events of virus interactions with DCs. Using this system and building on the results reported here, studies are under way to elucidate the mechanism(s) of binding and internalization of virus in immature versus mature DC subsets, including defining the receptors and uptake systems involved. In addition, the specific intracellular location of internalized virus and the subsequent fate of the virions in different DC subsets are being investigated. These studies should help to clarify the underlying mechanisms of retention of virus and subsequent transmission to T cells through which DCs have been proposed to amplify virus propagation. Despite the somewhat artificial conditions of exposing in vitro-cultured cells to relatively large amounts of purified virus, these studies should also provide important insights into how the virus is processed by the different DCs for Ag presentation and immune activation, allowing assessment of the functional significance of the differential postentry processing described here, with important ramifications for the development of DC-based vaccine approaches.

ACKNOWLEDGMENTS

We thank Loreley A. Villamide, Erin R. Mehlhop, John Santos, and Christine Santisteban for technical assistance; Larry Arthur and Julian Bess, Jr., of the AIDS Vaccine Program, SAIC Frederick, for the AT-

2-inactivated virus preparations; Ronald C. Desrosiers for providing SIVmac239; James Hoxie for providing SIVmac239/251 tail; Raoul Benveniste for providing SIVmneE11S; William C. Olson for providing the biotinylated CD4-IgG2; Judy Adams for help with computer graphics; and Ralph M. Steinman for critical review of the manuscript. We are also indebted to the veterinary and support staff, including Agegnehu Gettie, James Blanchard, Richard Rockar, and Marion Ratteree, at the Tulane Regional Primate Research Center for expert care and handling of the monkeys.

This work was supported by grants from the National Institutes of Health (AI47681), the Elizabeth Glaser Pediatric AIDS Foundation, The Rockefeller Foundation, and the Irma T. Hirschl Trust (to M.P.), as well as by the Erwin Schroedinger Fellowship funded by the Austrian government (to I.F.). This project has been funded in part with federal funds from the National Cancer Institute, National Institutes of Health, under contract no. NO1-CO-56000 (to J.D.L.).

REFERENCES

1. **Allaway, G. P., K. L. Davis-Bruno, G. A. Beaudry, E. B. Garcia, E. L. Wong, A. M. Ryder, K. W. Hasel, M. C. Gauduin, R. A. Koup, J. S. McDougal, et al.** 1995. Expression and characterization of CD4-IgG2, a novel heterotetramer that neutralizes primary HIV type 1 isolates. AIDS Res. Hum. Retrovir. **11:**533–539.
2. **Arthur, L. O., J. W. Bess, Jr., E. N. Chertova, J. L. Rossio, M. T. Esser, R. E. Benveniste, L. E. Henderson, and J. D. Lifson.** 1998. Chemical inactivation of retroviral infectivity by targeting nucleocapsid protein zinc fingers: a candidate SIV vaccine. AIDS Res. Hum. Retrovir. **14**(Suppl. 3)**:**S311–S319.
3. **Austyn, J. M.** 1996. New insights into the mobilization and phagocytic activity of dendritic cells. J. Exp. Med. **183:**1287–1292.
4. **Banchereau, J., and R. M. Steinman.** 1998. Dendritic cells and the control of immunity. Nature **392:**245–252.
5. **Barratt-Boyes, S. M., M. I. Zimmer, L. A. Harshyne, E. M. Meyer, S. C. Watkins, S. Capuano III, M. Murphey-Corb, L. D. Falo, Jr., and A. D. Donnenberg.** 2000. Maturation and trafficking of monocyte-derived dendritic cells in monkeys: implications for dendritic cell-based vaccines. J. Immunol. **164:**2487–2495.
6. **Benveniste, R. E., R. W. Hill, L. J. Eron, U. M. Csaikl, W. B. Knott, L. E. Henderson, R. C. Sowder, K. Nagashima, and M. A. Gonda.** 1990. Characterization of clones of HIV-1 infected HuT 78 cells defective in gag gene processing and of SIV clones producing large amounts of envelope glycoprotein. J. Med. Primatol. **19:**351–366.
7. **Bess, J. W., Jr., R. J. Gorelick, W. J. Bosche, L. E. Henderson, and L. O. Arthur.** 1997. Microvesicles are a source of contaminating cellular proteins found in purified HIV-1 preparations. Virology **230:**134–144.
8. **Blauvelt, A., H. Asada, M. W. Saville, V. Klaus-Kovtun, D. J. Altman, R. Yarchoan, and S. I. Katz.** 1997. Productive infection of dendritic cells by HIV-1 and their ability to capture virus are mediated through separate pathways. J. Clin. Investig. **100:**2043–2053.
9. **Cameron, P. U., M. G. Lowe, S. M. Crowe, U. O'Doherty, M. Pope, S. Gezelter, and R. M. Steinman.** 1994. Susceptibility of dendritic cells to HIV-1 infection in vitro. J. Leukoc. Biol. **56:**257–265.
10. **Desrosiers, R. C.** 1990. The simian immunodeficiency viruses. Annu. Rev. Immunol. **8:**557–578.
11. **Dezutter-Dambuyant, C., and D. Schmitt.** 1994. Epidermal Langerhans cells and HIV-1 infection. Immunol. Lett. **39:**33–37.
12. **Dybul, M., D. Weissman, A. Rubbert, E. Machado, M. Cohn, L. Ehler, M. O'Callahan, S. Mizell, and A. S. Fauci.** 1998. The role of dendritic cells in the infection of CD4+ T cells with the human immunodeficiency virus: use of dendritic cells from individuals homozygous for the Δ32CCR5 allele as a model. AIDS Res. Hum. Retrovir. **14:**1109–1113.
13. **Fackler, O. T., and B. M. Peterlin.** 2000. Endocytic entry of HIV-1. Curr. Biol. **10:**1005–1008.
14. **Feuerstein, B., T. G. Berger, C. Maczek, C. Roder, D. Schreiner, U. Hirsch, I. Haendle, W. Leisgang, A. Glaser, O. Kuss, T. L. Diepgen, G. Schuler, and B. Schuler-Thurner.** 2000. A method for the production of cryopreserved aliquots of antigen-preloaded, mature dendritic cells ready for clinical use. J. Immunol. Methods **245:**15–29.
15. **Garrett, W. S., L. M. Chen, R. Kroschewski, M. Ebersold, S. Turley, S. Trombetta, J. E. Galan, and I. Mellman.** 2000. Developmental control of endocytosis in dendritic cells by Cdc42. Cell **102:**325–334.
16. **Geijtenbeek, T. B. H., D. S. Kwon, R. Torensma, S. J. van Vliet, G. C. F. van Duijnhoven, J. Middel, I. L. M. H. A. Cornelissen, H. S. L. M. Nottet, V. N. KewalRamani, D. R. Littman, C. G. Figdor, and Y. van Kooyk.** 2000. DC-SIGN, a dendritic cell-specific HIV-1 binding protein that enhances *trans*-infection of T cells. Cell **100:**587–597.
17. **Geijtenbeek, T. B. H., R. Torensma, S. J. van Vliet, G. C. F. van Duijnhoven, G. J. Adema, Y. van Kooyk, and C. G. Figdor.** 2000. Identification of DC-SIGN, a novel dendritic cell-specific ICAM-3 receptor that supports primary immune responses. Cell **100:**575–585.
18. **Gorelick, R. J., R. E. Benveniste, T. D. Gagliardi, T. A. Wiltrout, L. K. Busch, W. J. Bosche, L. V. Coren, J. D. Lifson, P. J. Bradley, L. E. Henderson, and L. O. Arthur.** 1999. Nucleocapsid protein zinc-finger mutants of simian immunodeficiency virus strain mne produce virions that are replication defective in vitro and in vivo. Virology **253:**259–270.
19. **Granelli-Piperno, A., E. Delgado, V. Finkel, W. Paxton, and R. M. Steinman.** 1998. Immature dendritic cells selectively replicate macrophagetropic (M-tropic) human immunodeficiency virus type 1, while mature cells efficiently transmit both M- and T-tropic virus to T cells. J. Virol. **72:**2733–2737.
20. **Grewe, C., A. Beck, and H. R. Gelderblom.** 1990. HIV: early virus-cell interactions. J. Acquir. Immune Defic. Syndr. **3:**965–974.
21. **Hladik, F., G. Lentz, R. E. Akridge, G. Peterson, H. Kelley, A. McElroy, and M. J. McElrath.** 1999. Dendritic-cell–T-cell interactions support coreceptor-independent human immunodeficiency virus type 1 transmission in the human genital tract. J. Virol. **73:**5833–5842.
22. **Hu, J., M. B. Gardner, and C. J. Miller.** 2000. Simian immunodeficiency virus rapidly penetrates the cervicovaginal mucosa after intravaginal inoculation and infects intraepithelial dendritic cells. J. Virol. **74:**6087–6095.
23. **Hu, J., C. J. Miller, U. O'Doherty, P. A. Marx, and M. Pope.** 1999. The dendritic cell-T cell milieu of the lymphoid tissue of the tonsil provides a locale in which SIV can reside and propagate at chronic stages of infection. AIDS Res. Hum. Retrovir. **15:**1305–1314.
24. **Hu, J., M. Pope, U. O'Doherty, C. Brown, and C. J. Miller.** 1998. Immunophenotypic characterization of SIV-infected cells in cervix, vagina and draining lymph nodes of chronically infected rhesus macaques. Lab. Investig. **78:**435–451.
25. **Ignatius, R., F. Isdell, U. O'Doherty, and M. Pope.** 1998. Dendritic cells from skin and blood of macaques both promote SIV replication with T cells from different anatomical sites. J. Med. Primatol. **27:**121–128.
26. **Ignatius, R., M. Marovich, E. Mehlhop, L. Villamide, K. Mahnke, W. I. Cox, F. Isdell, S. S. Frankel, J. R. Mascola, R. M. Steinman, and M. Pope.** 2000. Canarypox virus-induced maturation of dendritic cells is mediated by apoptotic cell death and tumor necrosis factor alpha secretion. J. Virol. **74:**11329–11338.
27. **Ignatius, R., R. M. Steinman, A. Granelli-Piperno, D. Messmer, C. Stahl-Hennig, K. Tenner-Racz, P. Racz, I. Frank, L. Zhong, S. Schlesinger-Frankel, and M. Pope.** 2001. Dendritic cells during infection with HIV-1 and SIV, 2nd ed., p. 497–504. Academic Press, London, United Kingdom.
28. **Inaba, K., M. Inaba, M. Naito, and R. M. Steinman.** 1993. Dendritic cell progenitors phagocytose particulates, including bacillus Calmette-Guerin organisms, and sensitize mice to mycobacterial antigens in vivo. J. Exp. Med. **178:**479–488.
29. **Jiang, W., W. J. Swiggard, C. Heufler, M. Peng, A. Mirza, R. M. Steinman, and M. C. Nussenzweig.** 1995. The receptor DEC-205 expressed by dendritic cells and thymic epithelial cells is involved in antigen processing. Nature **375:**151–155.
30. **Jonuleit, H., U. Kuhn, G. Muller, K. Steinbrink, L. Paragnik, E. Schmitt, J. Knop, and A. H. Enk.** 1997. Pro-inflammatory cytokines and prostaglandins induce maturation of potent immunostimulatory dendritic cells under fetal calf serum-free conditions. Eur. J. Immunol. **27:**3135–3142.
31. **Lee, B., G. Leslie, E. Soilleux, U. O'Doherty, S. Baik, E. Levroney, K. Flummerfelt, W. Swiggard, N. Coleman, M. Malim, and R. W. Doms.** 2001. *cis* expression of DC-SIGN allows for more efficient entry of human and simian immunodeficiency viruses via CD4 and a coreceptor. J. Virol. **75:**12028–12038.
32. **Lifson, J. D., J. L. Rossio, M. Piatak, Jr., T. Parks, L. Li, R. Kiser, V. Coalter, B. Fisher, B. M. Flynn, S. Czajak, V. M. Hirsch, K. A. Reimann, J. E. Schmitz, J. Ghrayeb, N. Bischofberger, M. A. Nowak, R. C. Desrosiers, and D. Wodarz.** 2001. Role of $CD8^+$ lymphocytes in control of simian immunodeficiency virus infection and resistance to rechallenge after transient early antiretroviral treatment. J. Virol. **75:**10187–10199.
33. **Lutz, M. B., C. U. Assmann, G. Girolomoni, and P. Ricciardi-Castagnoli.** 1996. Different cytokines regulate antigen uptake and presentation of a precursor dendritic cell line. Eur. J. Immunol. **26:**586–594.
34. **Mahnke, K., M. Guo, S. Lee, H. Sepulveda, S. L. Swain, M. Nussenzweig, and R. M. Steinman.** 2000. The dendritic cell receptor for endocytosis, DEC-205, can recycle and enhance antigen presentation via MHCII+, lysosomal compartments. J. Cell Biol. **151:**673–683.
35. **Marechal, V., F. Clavel, J. M. Heard, and O. Schwartz.** 1998. Cytosolic Gag p24 as an index of productive entry of human immunodeficiency virus type 1. J. Virol. **72:**2208–2212.
36. **McDyer, J. F., M. Dybul, T. J. Goletz, A. L. Kinter, E. K. Thomas, J. A. Berzofsky, A. S. Fauci, and R. A. Seder.** 1999. Differential effects of CD40 ligand/trimer stimulation on the ability of dendritic cells to replicate and transmit HIV infection: evidence for CC-chemokine-dependent and -independent mechanisms. J. Immunol. **162:**3711–3717.
37. **Mehlhop, E., L. Villamide, I. Frank, A. Gettie, C. Santisteban, D. Messmer, R. Ignatius, J. D. Lifson, and M. Pope.** 2002. Enhanced activation of macaque dendritic cells induces strong immune T cell in vitro responses. J. Immunol. **260:**219–234.
38. **O'Doherty, U., R. Ignatius, N. Bhardwaj, and M. Pope.** 1997. Generation of monocyte-derived cells from the precursors in rhesus macaque blood. J. Immunol. Methods **207:**185–194.

39. **Pauza, C. D., and T. M. Price.** 1988. Human immunodeficiency virus infection of T cells and monocytes proceeds via receptor-mediated endocytosis. J. Cell Biol. **107:**959–968.
40. **Ploegh, H. L.** 1998. Viral strategies of immune evasion. Science **280:**248–253.
41. **Pope, M., M. G. H. Betjes, N. Romani, H. Hirmand, P. U. Cameron, L. Hoffman, S. Gezelter, G. Schuler, and R. M. Steinman.** 1994. Conjugates of dendritic cells and memory T lymphocytes from skin facilitate productive infection with HIV-1. Cell **78:**389–398.
42. **Pope, M., D. Elmore, D. Ho, and P. Marx.** 1997. Dendritic cell-T cell mixtures, isolated from the skin and mucosae of macaques, support the replication of SIV. AIDS Res. Hum. Retrovir. **13:**819–827.
43. **Pope, M., S. Gezelter, N. Gallo, L. Hoffman, and R. M. Steinman.** 1995. Low levels of HIV-1 in cutaneous dendritic cells promote extensive viral replication upon binding to memory CD4+ T cells. J. Exp. Med. **182:**2045–2056.
44. **Romani, N., G. Schuler, and P. Fritsch.** 1983. Distribution of anionic surface sites on human melanocytes and human melanoma cells in culture. Arch. Dermatol. Res. **275:**397–402.
45. **Rossio, J. L., M. T. Esser, K. Suryanarayana, D. K. Schneider, J. W. Bess, Jr., G. M. Vasquez, T. A. Wiltrout, E. Chertova, M. K. Grimes, Q. Sattentau, L. O. Arthur, L. E. Henderson, and J. D. Lifson.** 1998. Inactivation of human immunodeficiency virus type 1 infectivity with preservation of conformational and functional integrity of virion surface proteins. J. Virol. **72:**7992–8001.
46. **Sallusto, F., M. Cella, C. Danieli, and A. Lanzavecchia.** 1995. Dendritic cells use macropinocytosis and the mannose receptor to concentrate antigen in the major histocompatibility class II compartment. Downregulation by cytokines and bacterial products. J. Exp. Med. **182:**389–400.
47. **Sallusto, F., and A. Lanzavecchia.** 1994. Efficient presentation of soluble antigen by cultured human dendritic cells is maintained by granulocyte/macrophage colony-stimulating factor plus interleukin 4 and downregulated by tumor necrosis factor α. J. Exp. Med. **179:**1109–1118.
48. **Samson, M., F. Libert, B. J. Doranz, J. Rucker, C. Liesnard, C.-M. Farber, S. Saragosti, C. Lapoumeroulie, J. Cognaux, C. Forceille, G. Muyldermans, C. Verhofstede, G. Burtonboy, M. Georges, T. Imai, S. Rana, Y. Yi, R. J. Smyth, R. G. Collman, R. W. Doms, G. Vassart, and M. Parmentier.** 1996. Resistance to HIV-1 infection in caucasian individuals bearing mutant alleles of the CCR-5 chemokine receptor gene. Nature **382:**722–725.
49. **Stahl-Hennig, C., R. M. Steinman, K. Tenner-Racz, M. Pope, N. Stolte, K. Matz-Rensing, G. Grobschupff, B. Raschdorff, G. Hunsmann, and P. Racz.** 1999. Rapid infection of oral mucosal-associated lymphoid tissue with simian immunodeficiency virus. Science **285:**1261–1265.
50. **Turville, S. G., J. Arthos, P. U. Cameron, K. MacDonald, G. Clark, D. N. Hart, and A. L. Cunningham.** 2001. Bitter-sweet symphony: defining the role of dendritic cell gp120 receptors in HIV infection. J. Clin. Virol. **22:**229–239.
51. **Turville, S. G., J. Arthos, K. MacDonald, G. Lynch, H. Naif, G. Clark, D. N. Hart, and A. L. Cunningham.** 2001. HIV gp120 receptors on human dendritic cells. Blood **98:**2482–2488.
52. **Valladeau, J., V. Duvert-Frances, J. J. Pin, C. Dezutter-Dambuyant, C. Vincent, C. Massacrier, J. Vincent, K. Yoneda, J. Banchereau, C. Caux, J. Davoust, and S. Saeland.** 1999. The monoclonal antibody DCGM4 recognizes Langerin, a protein specific of Langerhans cells, and is rapidly internalized from the cell surface. Eur. J. Immunol. **29:**2695–2704.
53. **Valladeau, J., O. Ravel, C. Dezutter-Dambuyant, K. Moore, M. Kleijmeer, Y. Liu, V. Duvert-Frances, C. Vincent, D. Schmitt, J. Davoust, C. Caux, S. Lebecque, and S. Saeland.** 2000. Langerin, a novel C-type lectin specific to Langerhans cells, is an endocytic receptor that induces the formation of Birbeck granules. Immunity **12:**71–81.
54. **Werling, D., J. C. Hope, P. Chaplin, R. A. Collins, G. Taylor, and C. J. Howard.** 1999. Involvement of caveolae in the uptake of respiratory syncytial virus antigen by dendritic cells. J. Leukoc. Biol. **66:**50–58.
55. **Wu, L., A. A. Bashirova, T. D. Martin, L. Villamide, E. Mehlhop, A. O. Chertov, D. Unutmaz, M. Pope, M. Carrington, and V. N. KewalRamani.** Rhesus macaque dendritic cells transmit primate lentiviruses independently of DC-SIGN. Proc. Natl. Acad. Sci. USA, in press.
56. **Zhang, Y., B. Lou, R. B. Lal, A. Gettie, P. A. Marx, and J. P. Moore.** 2000. Use of inhibitors to evaluate coreceptor usage by simian and simian/human immunodeficiency viruses and human immunodeficiency virus type 2 in primary cells. J. Virol. **74:**6893–6910.
57. **Zhang, Z., T. Schuler, M. Zupancic, S. Wietgrefe, K. A. Staskus, K. A. Reimann, T. A. Reinhart, M. Rogan, W. Cavert, C. J. Miller, R. S. Veazey, D. Notermans, S. Little, S. A. Danner, D. D. Richman, D. Havlir, J. Wong, H. L. Jordan, T. W. Schacker, P. Racz, K. Tenner-Racz, N. L. Letvin, S. Wolinsky, and A. T. Haase.** 1999. Sexual transmission and propagation of SIV and HIV in resting and activated $CD4^+$ T cells. Science **286:**1353–1357.